

RESPONSES TO NRC QUESTIONS ON  
THE ROCS-DIT TOPICAL

CENPD-266

AMENDMENT 1-NP

February 1983

Nuclear Power Systems

C-E Power Systems

COMBUSTION ENGINEERING, INC.  
NUCLEAR POWER SYSTEMS  
POWER SYSTEMS GROUP  
WINDSOR, CONNECTICUT 06095

8304010511 830329  
PDR TOPRP EMVC-E  
C PDR

### Response to Question 1

Rod worths, ITC and critical ppm levels were calculated for the 3-D ANO-2 model with NEM in HERMITE and give results comparable to those with HOD in ROCS. In order to show those results, add the following before the last sentence at the end of Section 2.1.2 on page 2.23:

"Comparisons of rod worths, critical ppm and ITC for the 3-D ANO-2 model obtained using HERMITE (NEM) and ROCS (HOD) are given in Table 2.2. The critical ppm are essentially identical. The comparison also shows good agreement in bank worths with a maximum difference of [ ] between NEM and HOD. The bank worths with NEM give comparable agreement to measured values as seen by comparing the values with those in Table 4.18. The ITC agreement between NEM and HOD is also good. The comparison with measurement is given in Figure 4.2."

Replace Figure 4.2 by the attached Figure 4.2 and add a new Table 2.2 and renumber the current one as Table 2.3.

TABLE 2.2

COMPARISON OF NEM AND HOD REACTIVITY VALUES  
FOR ANO-2, BOC1 (3-D CALCULATIONS)

ROD WORTHS

<u>Sequential Rod Bank</u>	<u>HOD %Δρ</u>	<u>NEM %Δρ</u>	<u>Measured %Δρ</u>	<u>NEM-HOD % Difference</u>	<u>NEM-Measured % Difference</u>	<u>ROCS-Measured % Difference</u>
[ ]						

ITC (10<sup>-4</sup> Δρ/°F)

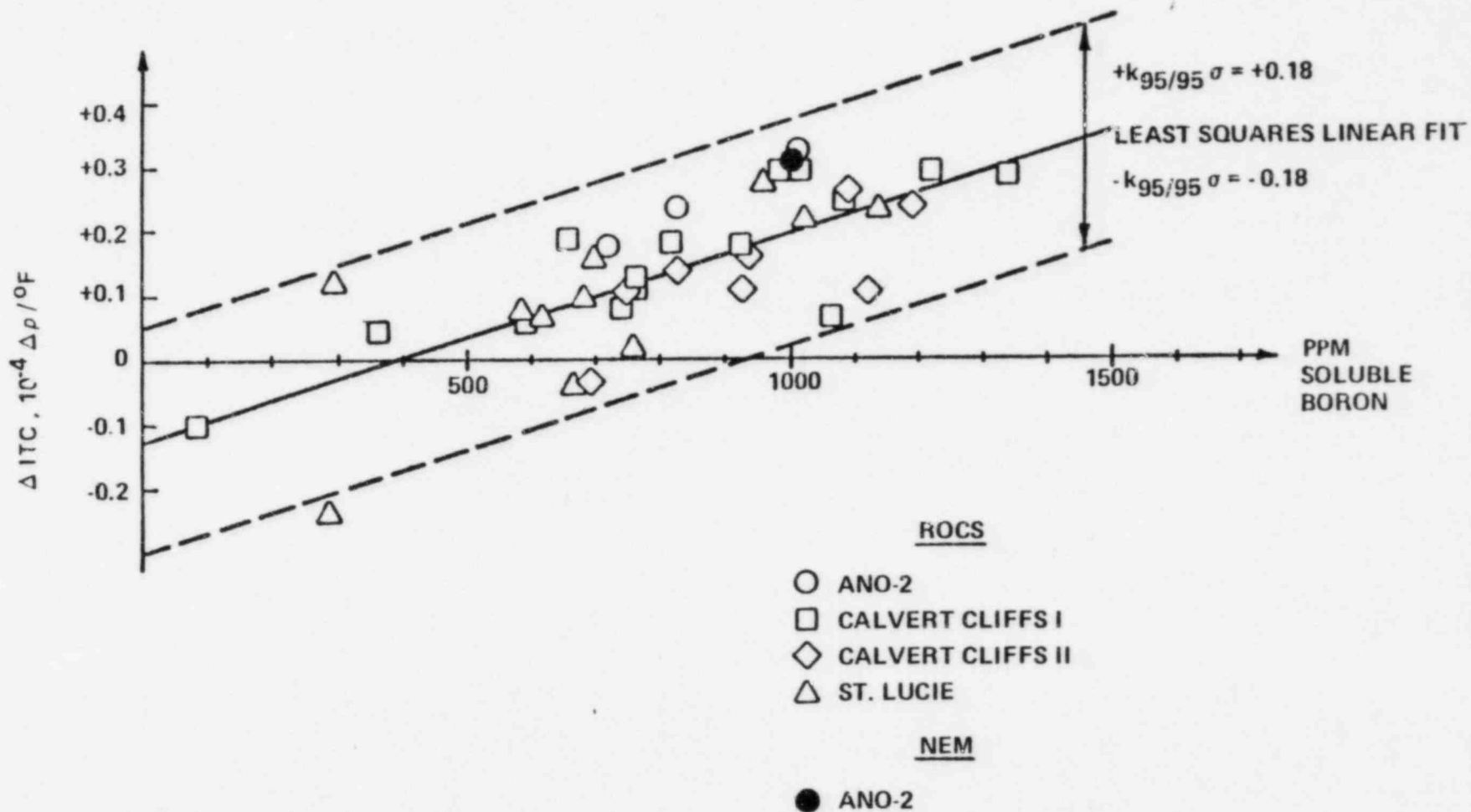
<u>HOD</u>	<u>NEM</u>	<u>Measured</u>	<u>NEM-HOD Δ ITC</u>	<u>NEM-Measured Δ ITC</u>	<u>ROCS-Measured Δ ITC</u>
[ ]					

Critical PPM (BOL equilibrium Xenon assumed)

<u>HOD</u>	<u>NEM</u>	<u>Measured</u>	<u>NEM-HOD</u>	<u>NEM-Measured</u>	<u>ROCS-Measured</u>
[ ]					

FIGURE 4-2

CALCULATION - MEASUREMENT ITC DIFFERENCE vs SOLUBLE BORON  
3D ROCS (DIT)



4.27

## Response to Question 2

If NEM were given the same macroscopic cross sections in both host codes, the results would be the same. The input cross section tables are the same in both ROCS and HERMITE. However, differences in macroscopic cross sections which would be used by NEM if it were in ROCS, compared to those it now uses in HERMITE, would arise because ROCS typically has four thermal hydraulic channels per assembly, while HERMITE typically uses one per assembly. An idea of the magnitude of this effect can be obtained from k-infinity maps given in figures 1, 2 and 3. These figures compare ROCS-HOD  $k_{\infty}$ 's to HERMITE-NEM  $k_{\infty}$ 's at BOC, MOC and EOC, and correspond to the power distributions in Figures 2-4, 5 and 6 in the topical. While the figures also reflect the different numerical methods in NEM and HOD, the  $k_{\infty}$ 's are quite close. The BOC HFP comparison is perhaps the most illuminating. The MOC and EOC comparisons show the added effect of depleting through one cycle with the slightly different power distributions. Thus, if NEM were put in ROCS, essentially the same results would be obtained as when NEM is run in HERMITE.

Figure 1  
2D MIDPLANE K-INFINITY COMPARISON  
NEM AND HOD AT BOC

Figure 2  
2D MIDPLANE K-INFINITY COMPARISON  
NEM AND HOD AT MOC

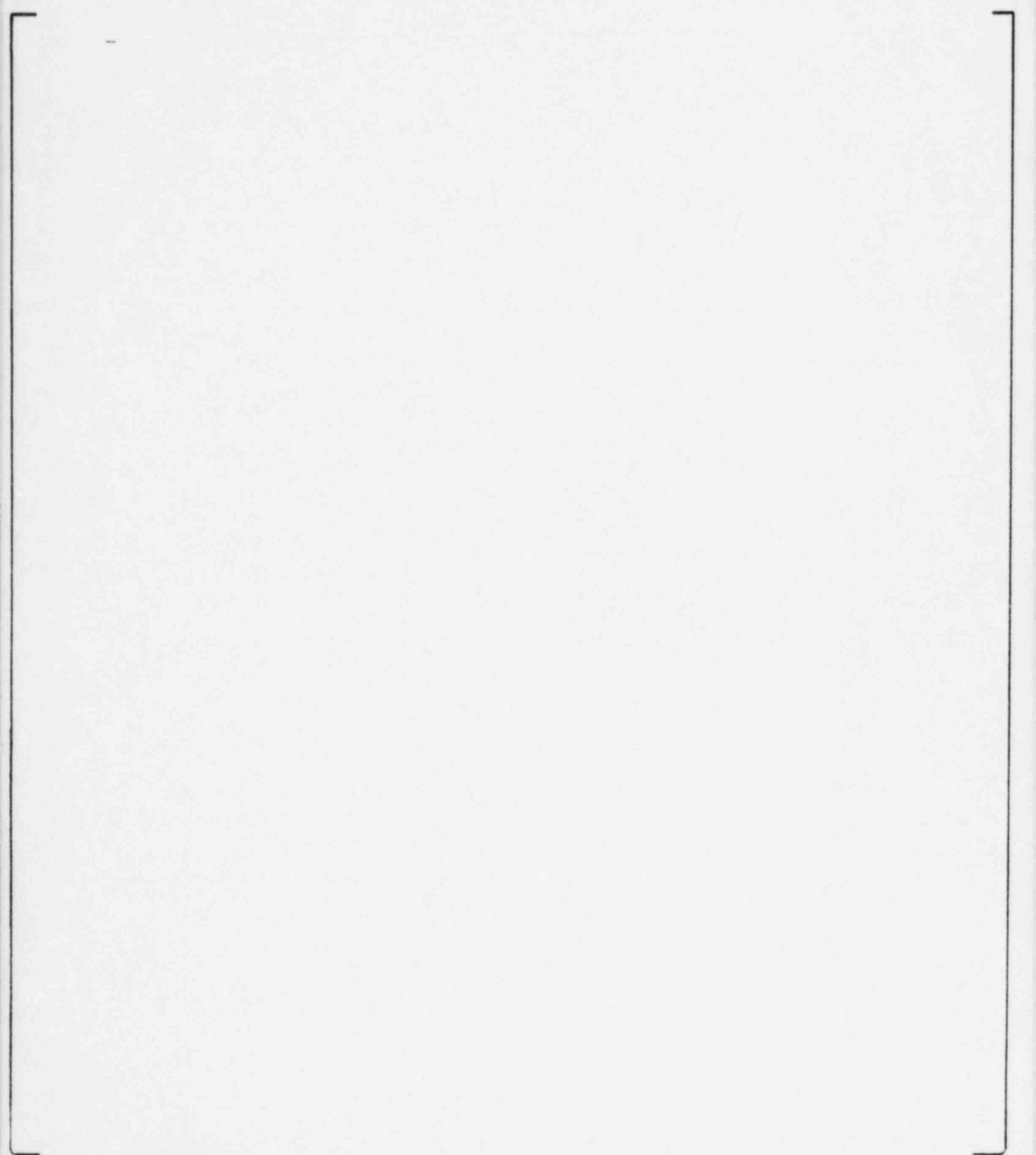


Figure 3  
2D MIDPLANE K-INFINITY COMPARISON  
NEM AND HOD AT EOC

### Response to Question 3

Comparisons showing the good agreement of CECOR coefficients generated by PDQ and ROCS/MC will be included. As part of this, replace the current Figures 2.14 through 2.17 with the following revised versions of Figures 2.14 through 2.17. Table 2.2 and Chapter 5 will be updated accordingly for the final submittal.<sup>+</sup> Then add the following section to 2.37.

#### "2.5.5 CECOR Coefficients

The CECOR program<sup>(2.17)</sup> for obtaining measured power distributions from in-core detector signals uses libraries of precalculated CECOR coefficients to convert detector signals into power distributions. The CECOR coefficients are a function of both the intra-assembly flux and pin-by-pin power distributions. These can be obtained from either PDQ or ROCS/MC. Both give essentially the same results.

"The CECOR pin-to-box factors relate the maximum pin power in an assembly to the average pin power in the assembly. Figures 2.14 through 2.17 in the preceding section give comparisons of the pin-to-box factors calculated by PDQ and by ROCS/MC. Maximum differences and standard deviations are on the order of [ - - - ].

"The CECOR W-PRIME factor which is the ratio of assembly power to rhodium activation in a detector is also a function of the local flux distribution within an assembly and within the water hole where the instrument resides. It is used to convert the instrument signal to the assembly power. Figures 2.18 through 2.20 compare W-PRIME factors calculated by PDQ and by ROCS and MC as a function of life. The results are essentially equivalent with standard deviations of the differences on the order of [ - - - ].

"The coupling coefficients which relate the power in uninstrumented boxes to powers in the instrumented boxes are a function of the overall global, inter-assembly power distributions. As Figures 2.4 through 2.6 in Section 2.1 show, power distributions calculated by PDQ and ROCS agree quite well. Figures 2.21 through 2.23 give a comparison of the resulting coupling coefficients as a function of life. The PDQ and ROCS values are essentially equivalent with standard deviations of the differences less than [ - - - ].

"CECOR coefficients are essentially the same whether they are obtained from PDQ or ROCS/MC. The use of one or the other affects the inferred power peaking on the order of [ - - - ]. This is significantly less than the 95/95 uncertainty of 5-6% assigned to CECOR."

---

<sup>+</sup> The final overall power peaking uncertainties for Fp, Fq, Fr and Fxy become .31, 5.16, 3.02, and 4.99%, respectively.

Figure 2-14  
COMPARISON OF PIN/BOX DIFFERENCES BETWEEN  
ROCS/MC AND PDQ  
BOC  
UNRODDED

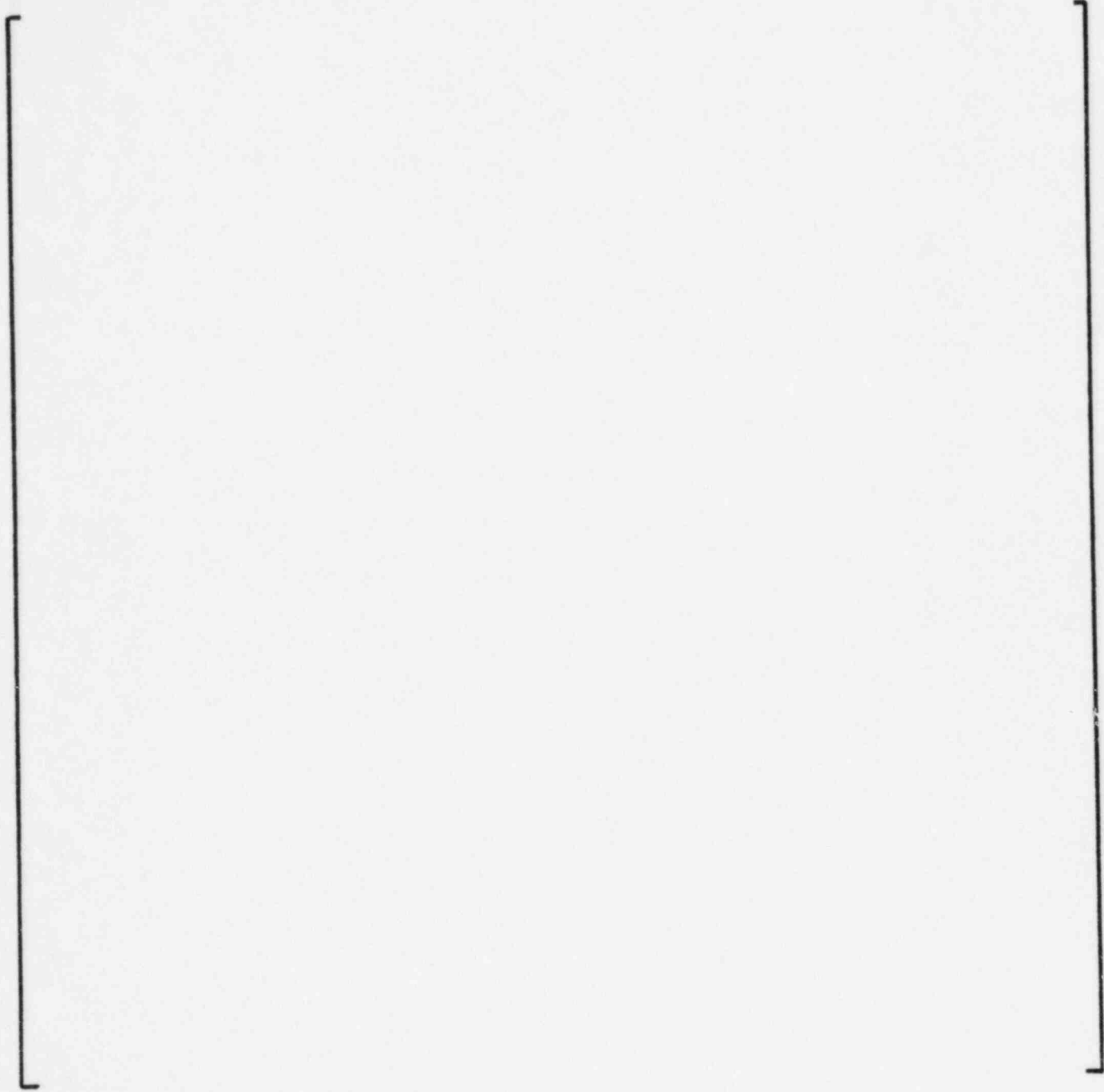


Figure 2-15  
COMPARISON OF PIN/BOX DIFFERENCES BETWEEN  
ROCS/MC AND PDQ  
MOC  
UNRODDED

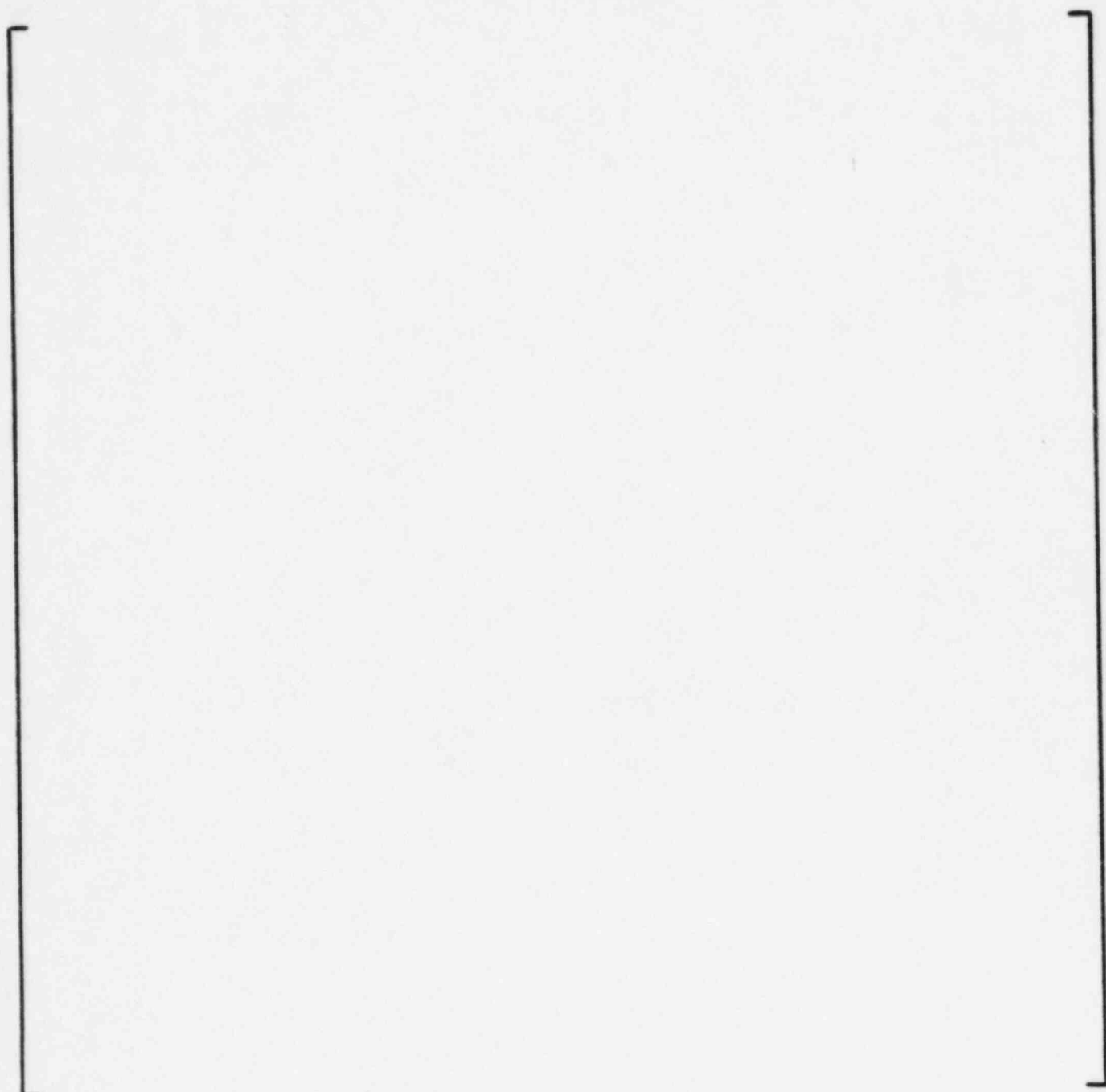


Figure 2-16  
COMPARISON OF PIN/BOX DIFFERENCES BETWEEN  
ROCS/MC AND PDQ  
EOC  
UNRODDED

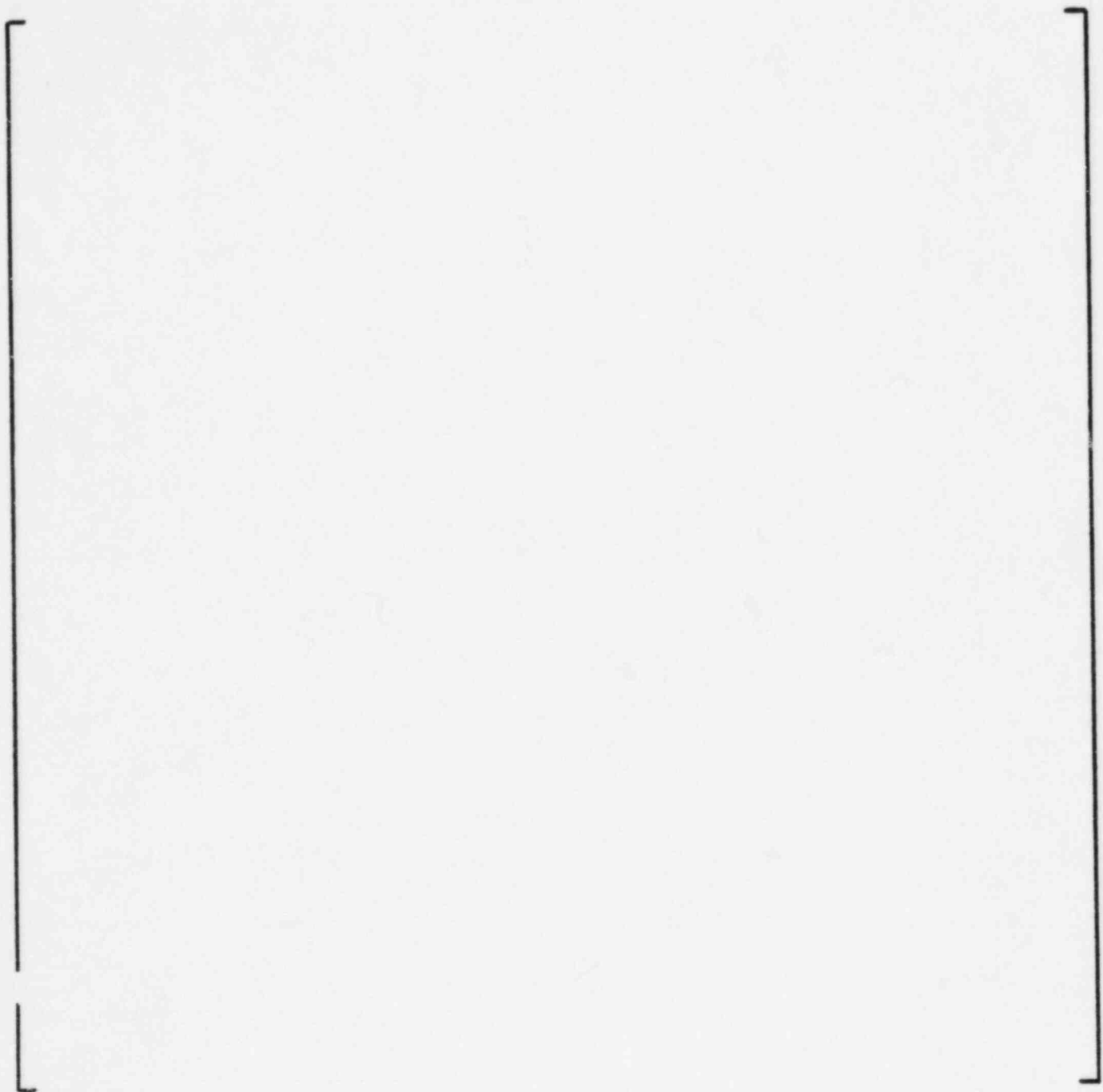


Figure 2-17  
COMPARISON OF PIN/BOX DIFFERENCES BETWEEN  
ROCS/MC AND PDQ  
BOC  
LEAD ROD BANK INSERTED

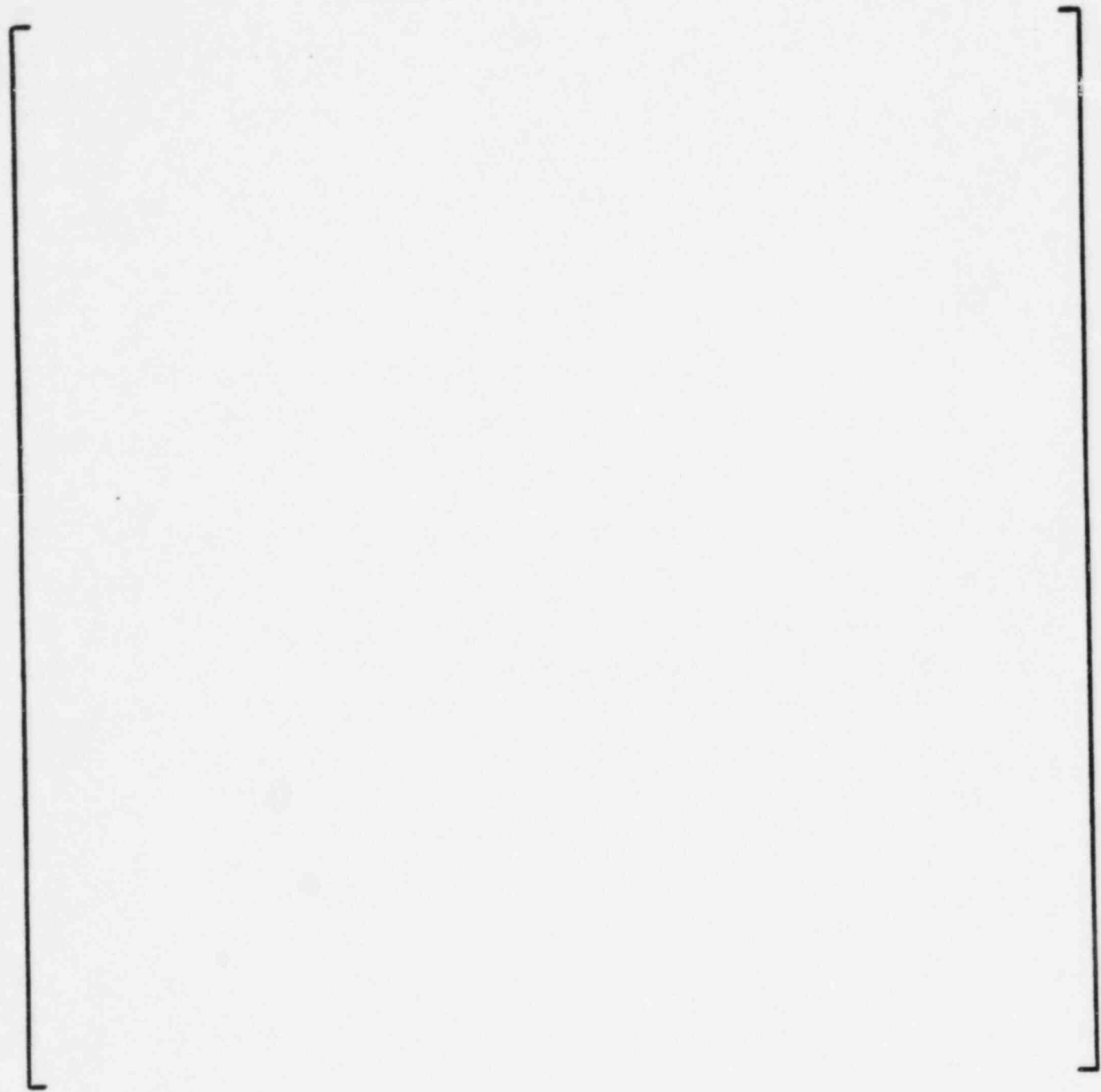


Figure 2-18  
COMPARISON OF W-PRIME DIFFERENCES BETWEEN  
ROCS/MC AND PDQ  
BOC

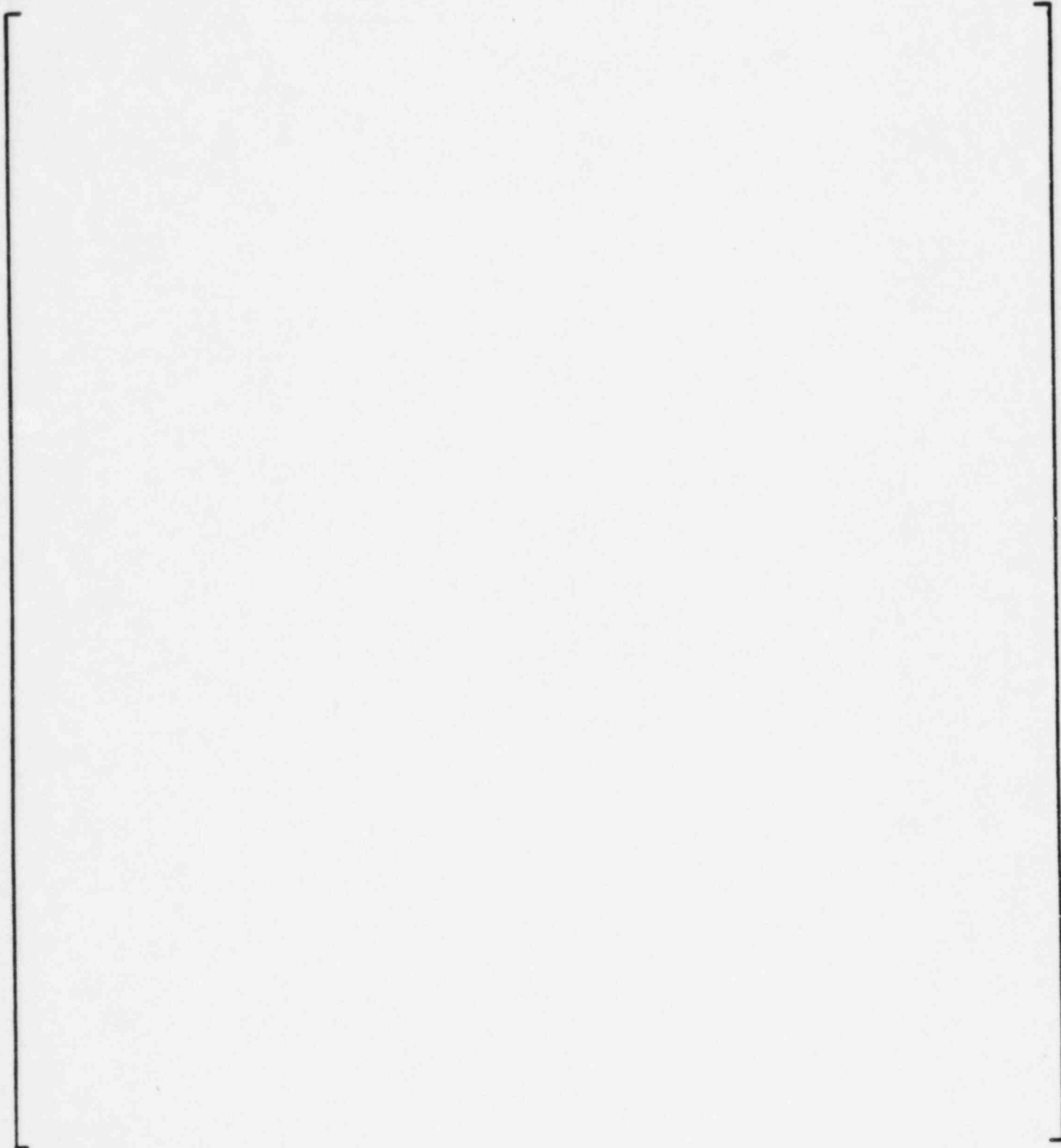


Figure 2-19  
COMPARISON OF W-PRIME DIFFERENCES BETWEEN  
ROCS/MC AND PDQ  
MOC

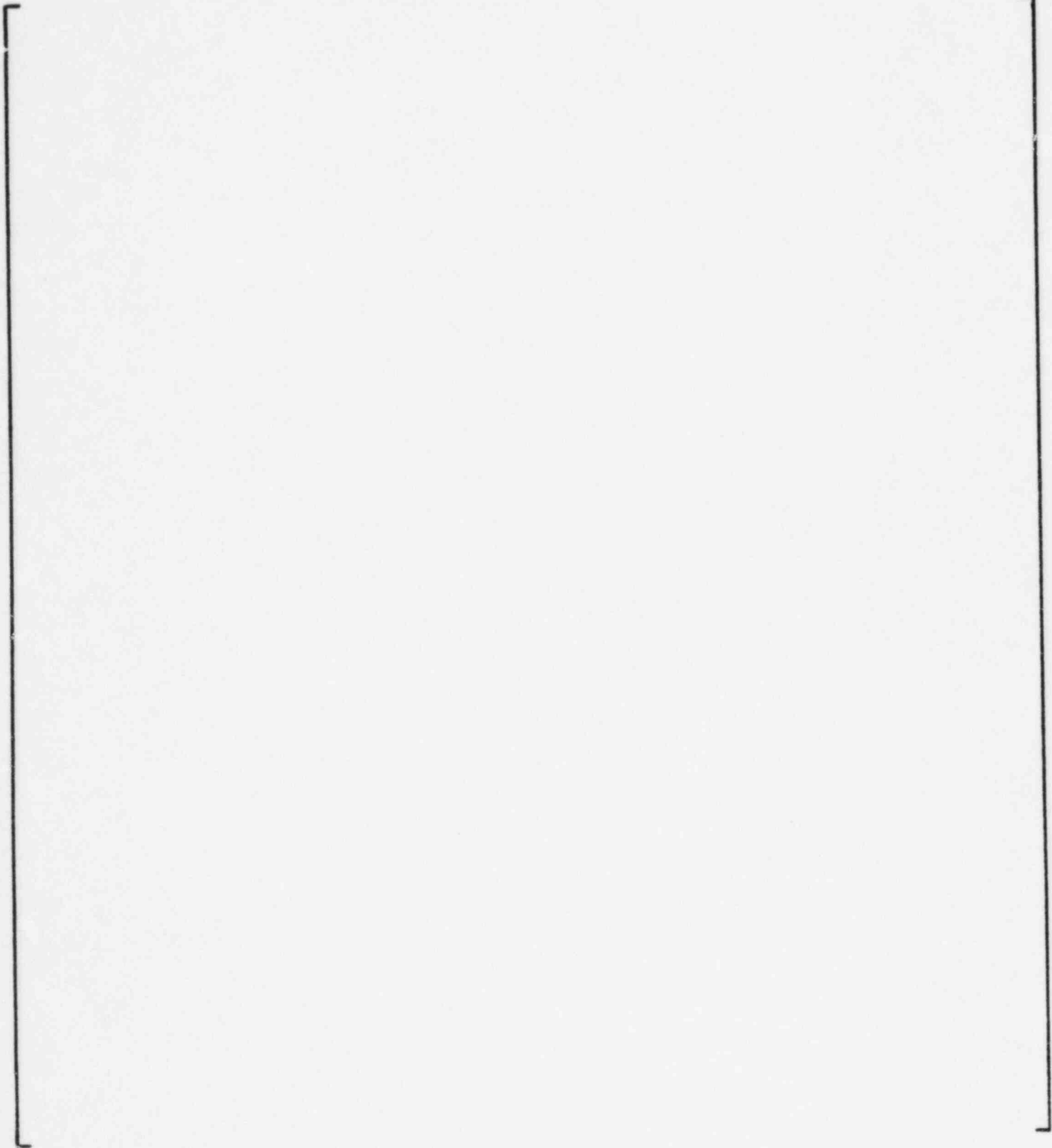


Figure 2-20  
COMPARISON OF W-PRIME DIFFERENCES BETWEEN  
ROCS/MC AND PDQ  
EOC

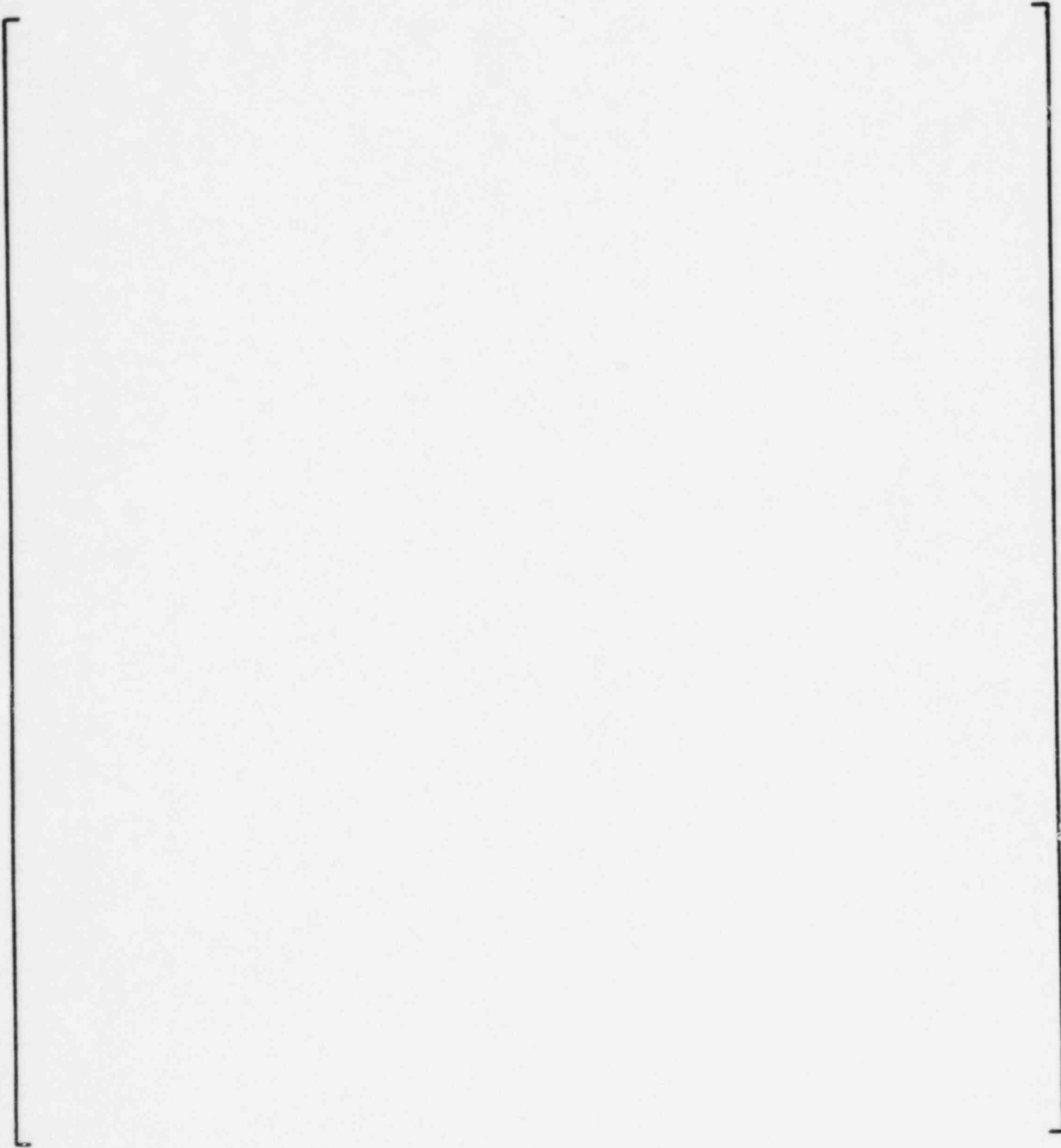


Figure 2-21  
COMPARISON OF COUPLING COEFFICIENT DIFFERENCES BETWEEN  
ROCS/MC AND PDQ  
BOC

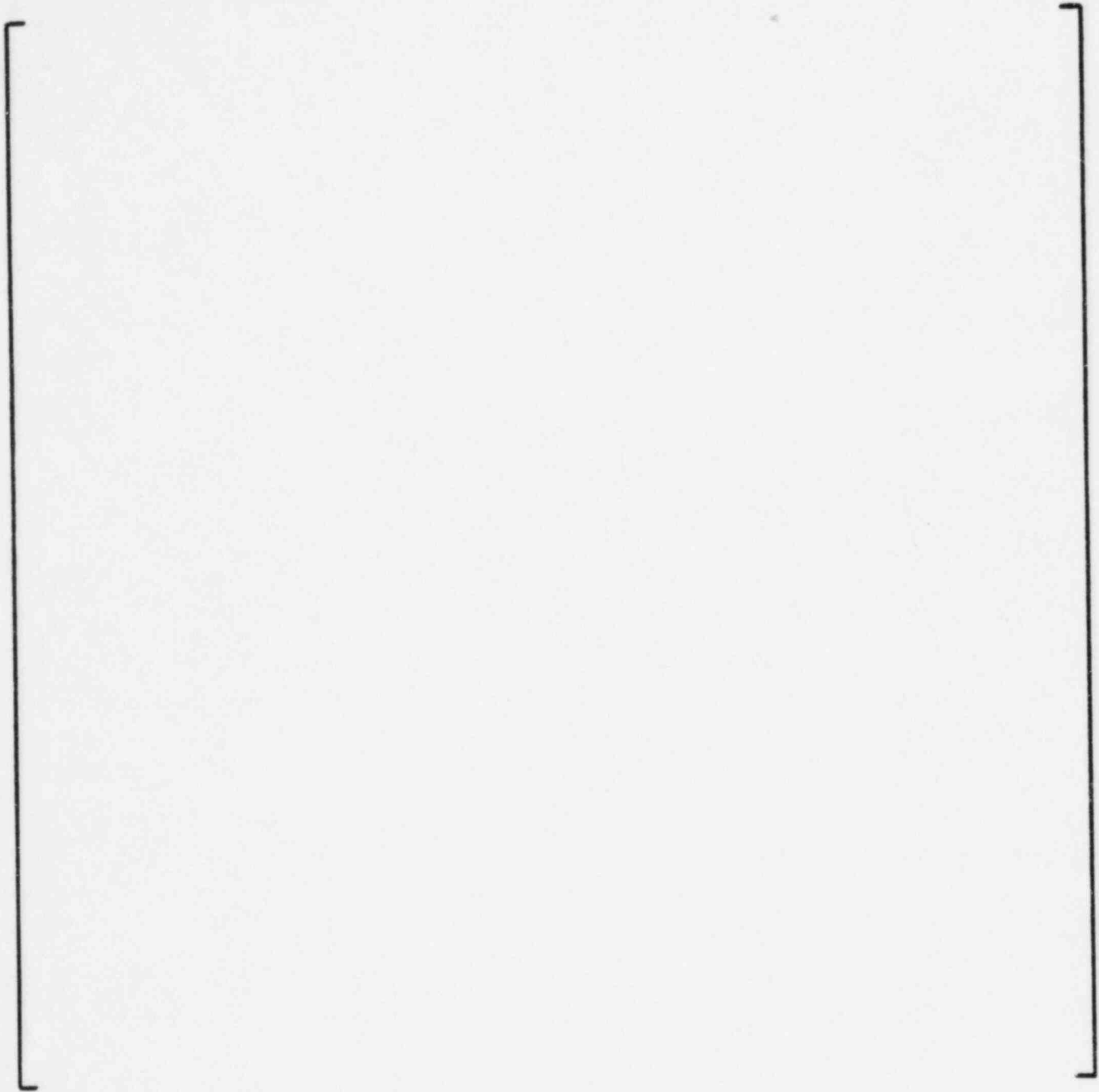


Figure 2-22

COMPARISON OF COUPLING COEFFICIENT DIFFERENCES BETWEEN  
ROCS/MC AND PDQ  
MOC

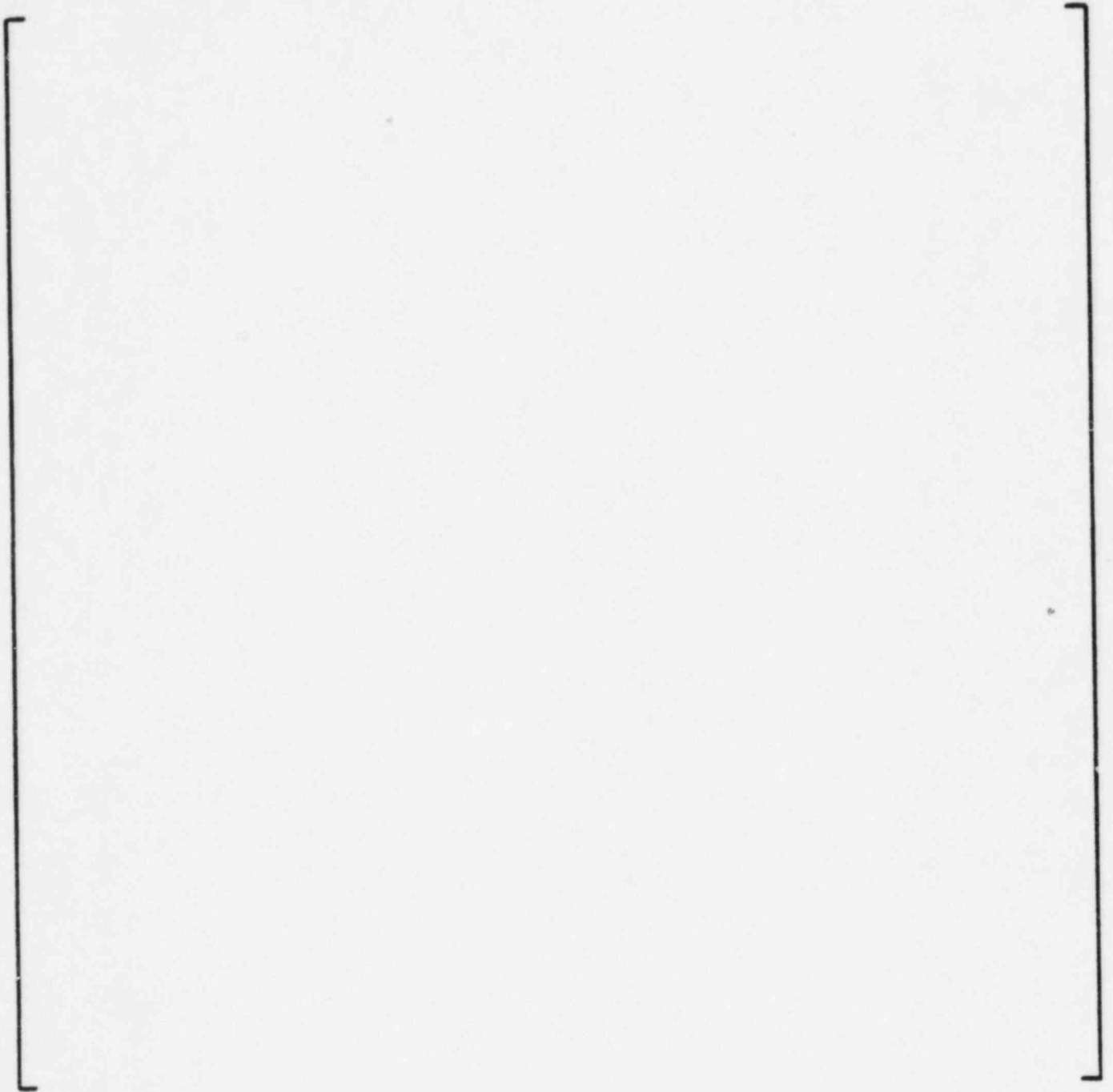
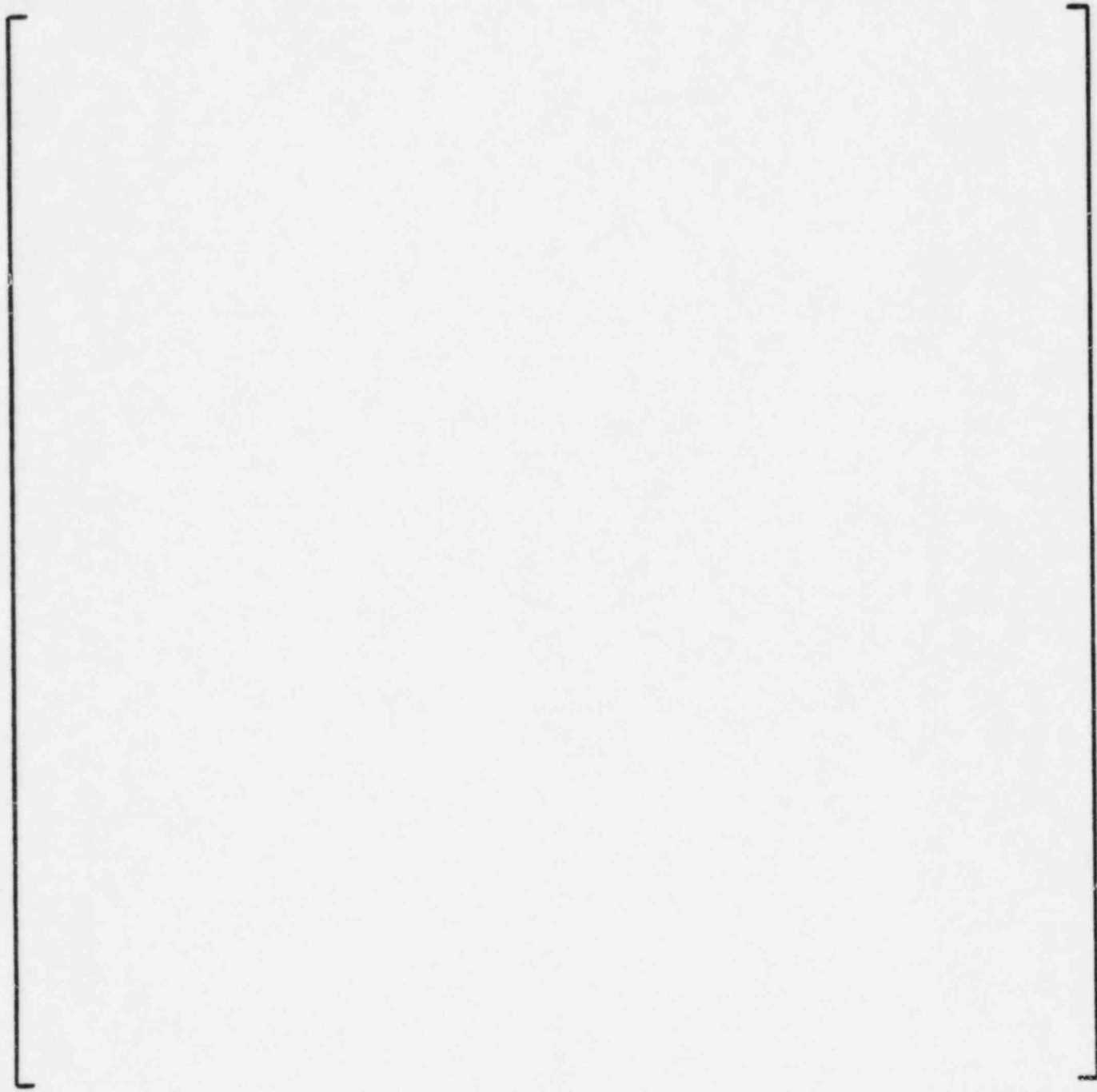


Figure 2-23  
COMPARISON OF COUPLING COEFFICIENT DIFFERENCES BETWEEN  
ROCS/MC AND PDQ  
EOC



Response to Question 4

Yes

Response to Question 5

The PDQ's explicitly represent the shroud, water and barrel. To clarify, add the following text after the second sentence on page 2.22:

"The fine-mesh, PDQ calculations explicitly represented the shroud, reflector, and barrel, [ ]."

#### Response to Question 6

The intent of Figures 2-4 through 2-6 was only to show a consistent set of 2-dimensional comparisons of PDQ, HOD, and NEM and the good agreement among the methods throughout life. If 2-dimensional planes other than the mid-plane had been used, the only modeling differences would be in the choice of planar power, temperature, and buckling. In design practice, when C-E performs 2-dimensional planar calculations, they are for the mid-plane, not a core average plane, since the midplane more accurately represents the radial power distribution throughout most of the core.

### Response to Question 7

Comparisons have been made of HERMITE (NEM) and ROCS (HOD) 3-D power distribution at full power as a function of life. The maximum differences do not exceed [     ]. To show these results, replace the last sentence on page 2.22 with the following.

"Figures 2.9 a-d show the standard deviations and maximum errors resulting from these radial comparisons between NEM and HOD as a function of axial position and life. Maximum differences are on the order of [     ]."

Further, rename the current Figure 2.9 as Figure 2.9a, and add Figures 2.9 b-e.

Figure 2-9b  
NEM-ROCS, RMS AND MAXIMUM PERCENT DIFFERENCES  
IN THE RADIAL POWER DISTRIBUTION vs PERCENT  
OF CORE HEIGHT

ANO-2 2625 MWD/T  
100% POWER

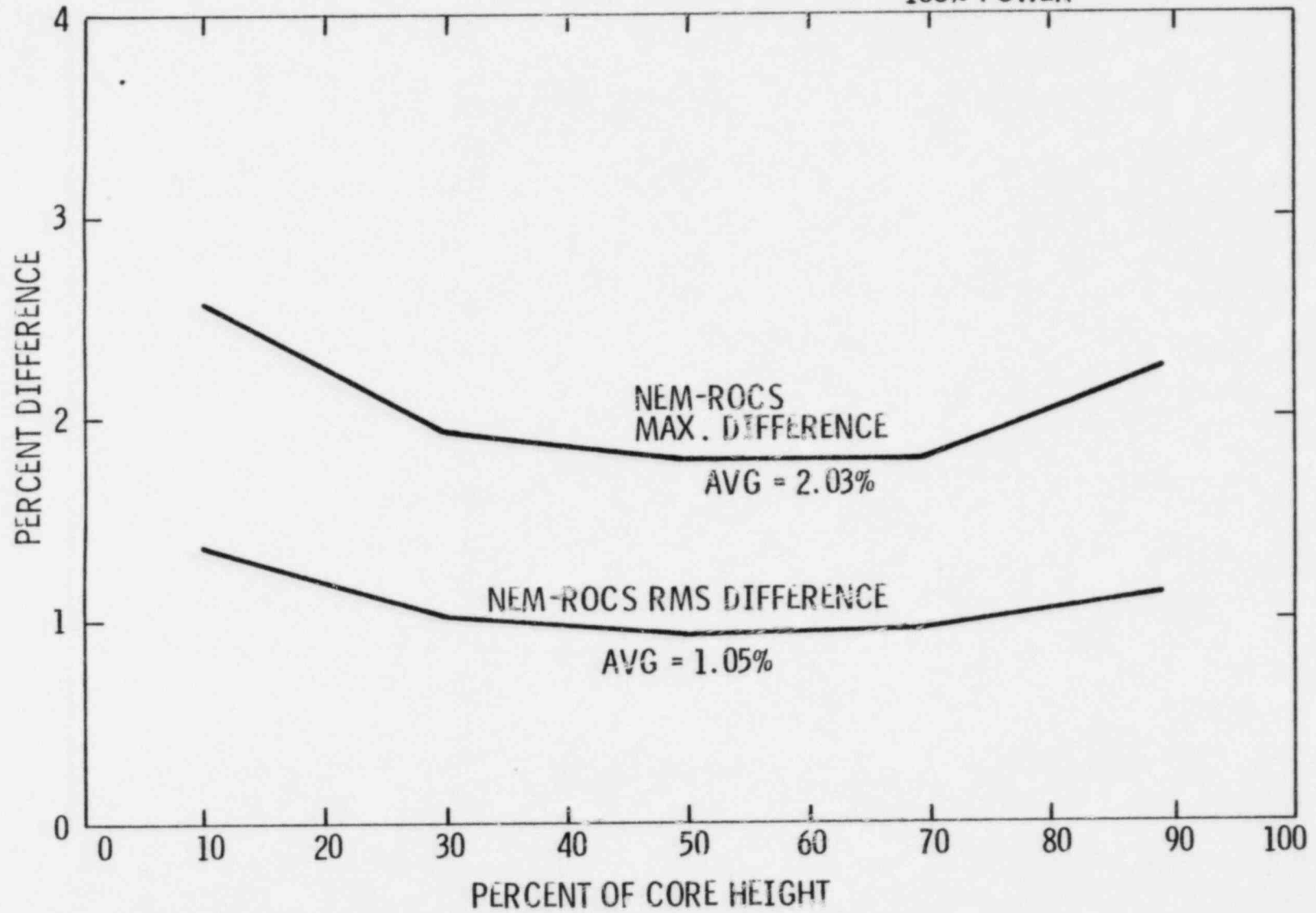


Figure 2-9c  
NEM-ROCS, RMS AND MAXIMUM PERCENT DIFFERENCES  
IN THE RADIAL POWER DISTRIBUTION vs PERCENT  
OF CORE HEIGHT

ANO-2 MOC 8290 MWD/T  
100% POWER

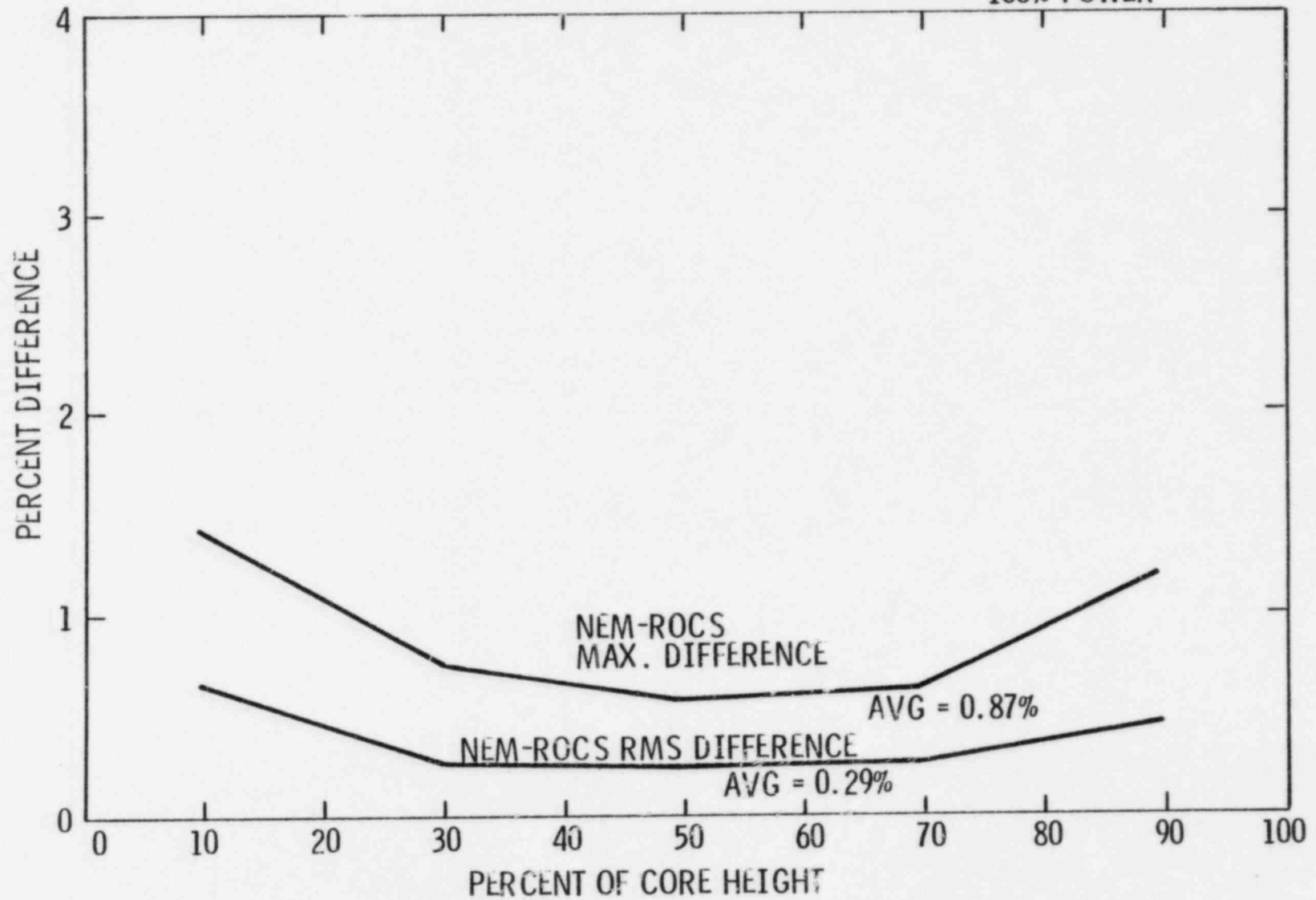
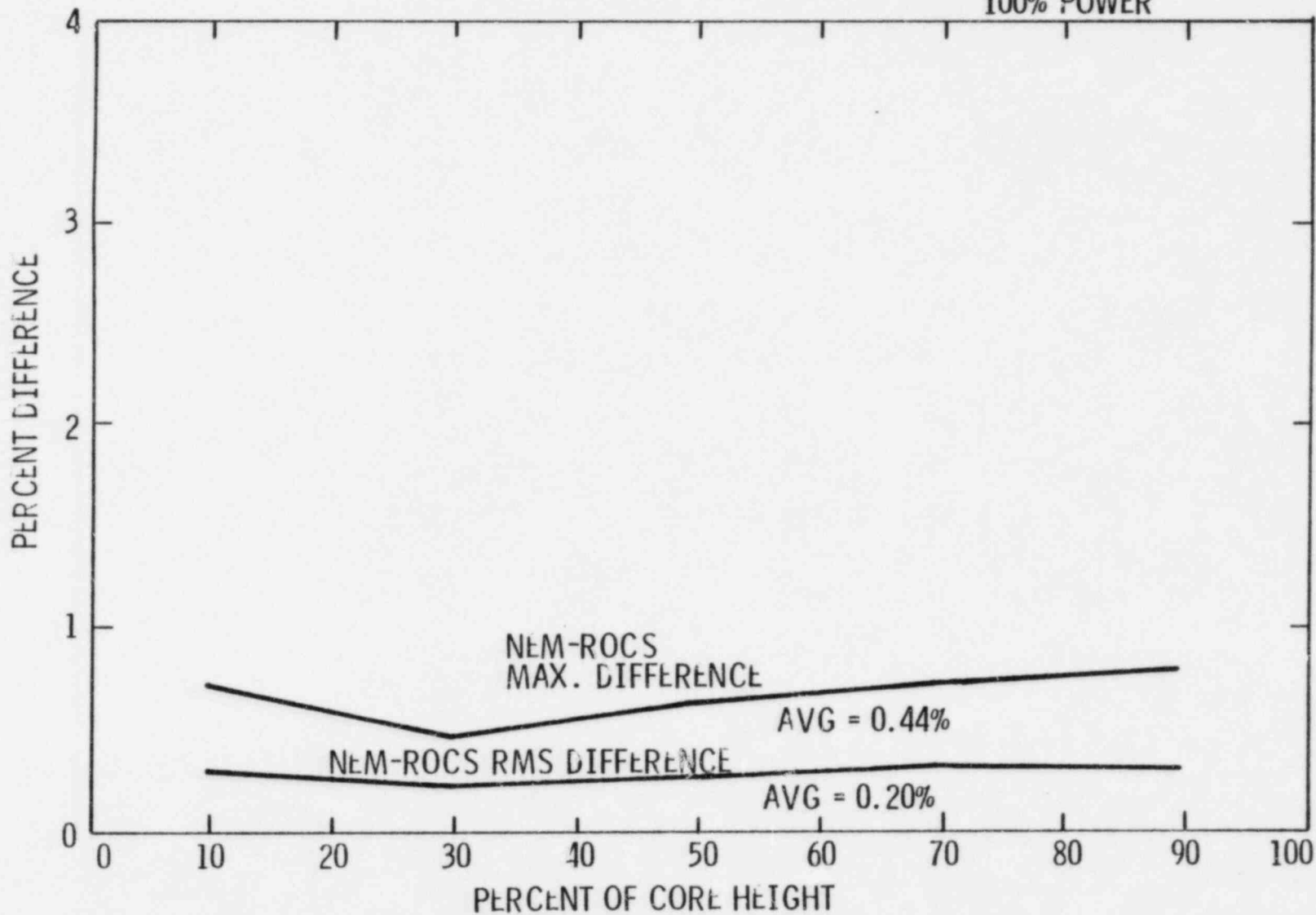


Figure 2-9d  
NEM-ROCS, RMS AND MAXIMUM PERCENT DIFFERENCES  
IN THE RADIAL POWER DISTRIBUTION vs PERCENT  
OF CORE HEIGHT

ANO-2 EOC 12450 MWD/T  
100% POWER



### Response to Question 8

The fuel temperature correlation in Reference 2.16 is still valid. As clarification, change the last sentence in last paragraph in Section 2.3 on page 2.30 to read:

"A detailed description of the development and verification of this fuel temperature correlation for power feedback and reactivity coefficient applications is given in Reference 2.16."

Then add the following:

"The power coefficient itself is a function of the change in fuel temperature with linear heat rate and the change in resonance integral through Doppler broadening with fuel temperature. A best estimate of the fuel temperature is obtained from the FATES code as a function of linear heat rate and fuel exposure for each fuel type contained in the core. Each fuel type is characterized by its heat transfer and densification/relocation properties. The three principal fuel types which have been considered are:

1. Densifying fuel, air filled, unpressurized.
2. Non-densifying, Helium filled, unpressured.
3. Non-densifying, Helium filled, pressurized.

"The fuel temperature correlations have been constructed with the FATES results for each fuel type, and are used accordingly in ROCS. The fuel enrichment and soluble boron level have a negligible effect on the fuel temperature at a given linear heat rate, since the temperature is primarily a function of the fuel heat transfer properties."

"The Doppler broadening is explicitly accounted for in DIT during the spectrum calculation and generation of broad group cross sections. [

Since they are implemented in ROCS on a microscopic basis for each nuclide and ROCS calculates the fuel temperature, there is no restriction based on the applicable range of enrichment and soluble boron." ]

Further on page 2-39, change the last line of Reference 2-16 to read:

Application," Trans. Am. Nucl. Soc. 30 , 715, 1978 and Combustion Engineering Report TIS-6021."

Response to Question 9

The intent of Figure 2-13 was to show the applicability of D's calculated by the standard procedure for cases other than those for which they were calculated. To clarify this, add the following text after the third sentence in the second paragraph on page 2.36.

"Thus, the results in Figure 2.13 also show the applicability of using diffusion coefficients obtained from DIT's, with zero net external leakage, in MC for cases with strong gradients accross an assembly."

Further, change the last sentence in the second paragraph to read:

"This close agreement between MC and transport theory fission rates illustrates the accuracy of the assumption of univ ersially applicable diffusion coefficients even for cases for which they were not explicitly calculated."

### Response to Question 10

Currently the 85-group library is used in DIT production runs. However, the 41-group library will be used in the future. The two libraries give essentially the same results in PWR design analyses. To clarify this, replace the last paragraph in Section 3.3.5 on page 3.11 with the following:

"The 41-group library has been tested against the basic 85-group library which is currently used in design applications and has been shown to accurately reproduce reactivity levels, reactivity coefficients, power distributions and reaction rates. In PWR assembly calculations the differences in individual reaction rates are on the order of [ ] in magnitude for the two libraries. Infinite multiplication factors differ on the order of [ ] over a normal depletion range."

Response to Question 11

The special capabilities of ROCS and DIT which enable them to model the unique features of gadolinia will be described. To do this for ROCS, add the following text to Section 2.2.2 on page 2-27 after the last sentence.

"[

]"

The modeling of gadolinia in DIT makes use of existing capabilities in the code which enable detailed calculation of the flux and spectrum in the gadolinia pins and surrounding assembly. These include use of heterogeneous geometry for both spectrum and assembly calculations, increased radial subdivisions for gadolinia pins, azimuthal flux variation in the vicinity of Gd and waterholes, and use of an appropriate broad energy group structure for the assembly calculation (See Figure 1 attached).

A new capability was added to the DIT depletion calculation to enable use of normal time stepping for fuel assemblies with gadolinia without loss of accuracy relative to use of very fine time steps. In order to better describe the modeling of gadolinia, modify the third to last sentence in Section 3-4-1 on page 3.12 to read:

"The boron chain is a simple depletion of  $^{10}\text{B}$ , while the Gd chains use the [ ] method described in the following section."

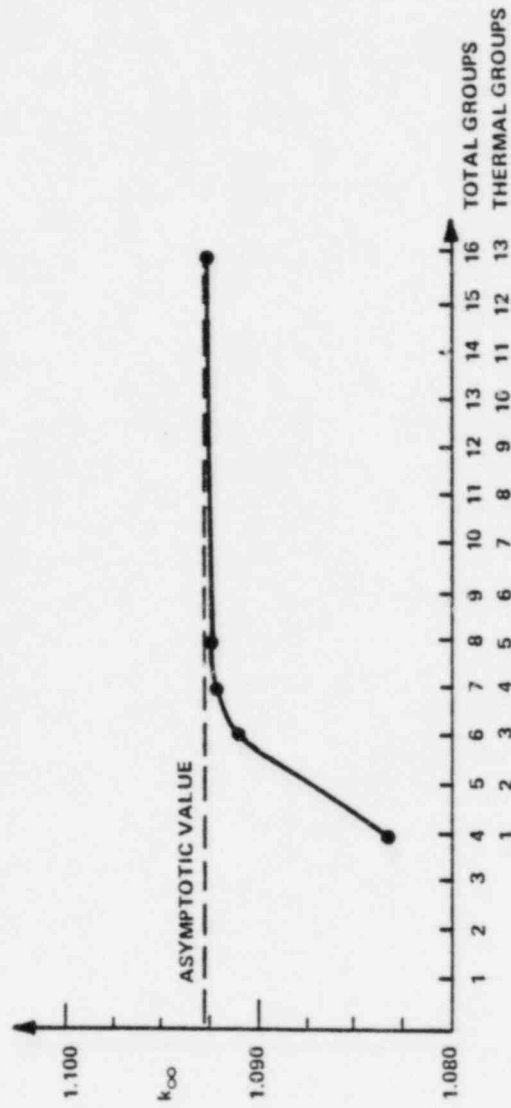
Further, add the following discussion at the end of section 3-4-2 on page 3.15:

"In depletion of fuel loaded with Gd, the high cross-sections of Gd-155 and Gd-157 lead to a rapid variation of the flux level in the fuel pins. Since the flux level and the spectrum are assumed to be constant during a time step in the method described above, very frequent recalculations (typically 50-100 hour timesteps) of the flux would be necessary if it were applied to Gd depletion without modification. In order to maintain time step lengths that are manageable, [

]. This method has been tested against direct calculations with very short timesteps.

"Another feature of DIT which is important for the depletion of Gd is that a Gd pin, apart from an increased number of subdivisions in the pin, each of which deplete individually, is treated in the same way as any other type of pin. No separate, auxiliary calculations are employed in order to form cell averaged cross-sections. This is possible because DIT performs the assembly calculation, from which the flux distribution for the depletion comes, without homogenizing the geometry."

FIGURE 1  
 SENSITIVITY OF  $k_{\infty}$  vs ASSEMBLY GROUP STRUCTURE  
 16 x 16 ASSEMBLY WITH 16  $Gd_2O_3/UO_2$  SHIMS AT 2 Wt%  $Gd$  LOADING



## Response to Question 12

The ROCS calculations were depleted in a core-follow mode, modeling the actual depletion history. The ROCS depletion structure for each cycle will be given. To accomplish this, change the last sentence in the second paragraph on page 4-7 to read:

"These depletions incorporated details of power level, control rod insertion, inlet water temperature and soluble boron operating histories using several time-steps per 1000 MWD/T of core burnup, where needed to model changes in these parameters. The ROCS depletion structure for the eight cycles is given in Tables 4-2 through 4-9."

TABLE 4.2  
 ROCS MANEUVER STRUCTURE  
 ANO-2 CYCLE 1

Maneuver No.	Burnup (MWD/T)	Percent Power	PPM	Bank	Rod Position % In	Inlet Temp. °F
0	0	20	868		ARO	546
1	272	50	722		ARO	551
2	356	50	722		ARO	551
3	686	50	725		ARO	551
4	859	50	719	6	20.	551
5	915	50	726		ARO	551
6	1150	51	727		ARO	552
7	1470	51	728		ARO	552
8	1775	78	676		ARO	553
9	1980	78	661		ARO	553
10	2185	52	722	6	25.	548
11	2380	100	611		ARO	554
12	2625	100	596	6	12.	554
13	2730	100	606		ARO	554
14	3210	80	621		ARO	552
15	3675	80	575	6	7.5	552
16	3915	89	575	6	5.	552
17	4380	100	545	6	11.	554
18	4720	100	525	6	10.	554
19	5020	100	510	6	11.	554

TABLE 4.3

ROCS MANEUVER STRUCTURE  
CALVERT CLIFFS I CYCLE 1

Maneuver No.	Burnup (MWD/T)	Percent Power	PPM	Rod Position Bank	% In	Inlet Temp. °F
0	0	20	900	ARO		535
1	100	50	820	ARO		537
2	500	80	773	ARO		539
3	850	100	754	ARO		544
4	1000	100	745	ARO		544
5	2000	100	747	ARO		544
6	3000	100	735	ARO		544
7	4000	100	710	ARO		544
8	5000	100	680	ARO		544
9	6000	100	640	ARO		544
10	7000	100	590	ARO		544
11	8000	100	545	ARO		544
12	9000	100	490	ARO		544
13	10000	100	432	ARO		544
14	11000	100	365	ARO		544
15	12000	100	300	ARO		544
16	13000	100	235	ARO		544
17	14000	100	165	ARO		544
18	15000	100	90	ARO		544
19	15500	100	50	ARO		544
20	16000	95	17	5	18.	545
21	16526	68	21	5	18.	542
22	16672	57	30	5	18.	540
23	17000	57	30	5	18.	540
24	17100	57	30	5	18.	540

TABLE 4.4

ROCS MANEUVER STRUCTURE  
CALVERT CLIFFS I CYCLE 2

Maneuver No.	Burnup (MWD/T)	Percent Power <sup>+</sup>	PPM	Rod Position Bank	% In	Inlet Temp. °F
0	0	49.	763	5	23.	537
1	75	70.	713		ARO	540
2	150	80.	704		ARO	540
3	200	90.	660		ARO	545
4	325	100.	618		ARO	545
5	990	100.	580		ARO	545
6	1436	100.	550		ARO	545
7	1746	100.	530		ARO	545
8	2087	100.	492		ARO	545
9	2722	100.	444		ARO	545
10	3341	100.	394		ARO	545
11	3970	100.	345		ARO	545
12	4192	100.	332		ARO	545
13	5056	101.6	258		ARO	545
14	6000	101.6	182		ARO	545
15	6446	103.9	140		ARO	545
16	7000	102.6	91		ARO	547
17	7360	103.5	68		ARO	547
18	7600	101.9	24		ARO	547
19	8280	94.4	16	5	3.2	536
20	8330	94.4	15	5	3.2	536

<sup>+</sup>Based on nominal power of 2560 MW.

TABLE 4.5

ROCS MANEUVER STRUCTURE  
CALVERT CLIFFS II CYCLE 1

Maneuver No.	Burnup (MWD/T)	Percent Power <sup>+</sup>	PPM	Bank	Rod Position % In	Inlet Temp. °F
0	0	50.	830		ARO	540.
1	200	80.	785		ARO	542.5
2	325	100.	772		ARO	542.5
3	400	100.	740		ARO	545.
4	650	100.	750	5	25.	545.
5	1000	100.	755		ARO	545.
6	1438	100.	759		ARO	545.
7	2473	100.	751		ARO	545.
8	3331	0.	730		ARO	545.
9	3331	100.	730		ARO	545.
10	4088	100.	706		ARO	545.
11	4400	100.	696		ARO	555.
12	5000	100.	676		ARO	545.
13	5631	100.	656		ARO	545.
14	6230	100.	637		ARO	545.
15	6880	100.	615		ARO	545.
16	7435	100.	593		ARO	545.
17	8261	105.37	544	5	2.56	545.
18	8751	105.47	514	5	2.56	546.
19	9169	95.30	484	5	10.24	546.
20	9983	103.40	433	5	5.12	546.
21	10205	102.60	426	5 <sup>++</sup>	5.12	546.
22	10675	102.70	410	5	5.12	546.
23	11116	97.0	378	5	5.12	546.
24	11979	103.4	328	5	5.12	546.
25	12369	78.0	345	5	5.12	542.
26	12837	71.7	324	5	5.12	542.
27	12959	105.47	266	5	5.12	546.
28	12959	71.7	306	5	5.12	542.
29	13283	71.7	284	5	5.12	542.
30	13811	71.7	247	5	5.12	542.
31	13811	74.14	246	5	5.12	542.
32	14313	65.88	223	5	7.68	543.5
33	15185	90.49	123	5	7.68	543.5
34	15525	90.98	97	5	7.68	545.5
35	16182	90.98	45	5	7.68	545.5

+ Based on nominal power of 2560 MW.

++ All other rods were at 3.4% insertion for the rest of cycle.

TABLE 4.6

ROCS MANEUVER STRUCTURE  
CALVERT CLIFFS II CYCLE 2

Maneuver No.	Burnup (MWD/T)	Percent Power	PPM	Bank	Rod Position % In	Inlet Temp. °F
0	0	48.71	960	5	2.0	541.
1	33	80.80	946	5	2.0	543.
2	200	94.	881	5	2.0	543.
3	280	87.54	840	5	9.0	543.5
4	389	87.14	820	5	8.0	542.
5	558	97.	815	5	9.0	547.
6	809	97.30	790		ARO	546.
7	1273	97.10	740	5	23.0	546.
8	1438	98.20	735		ARO	546.
9	1698	98.20	705	5	8.4	546.
10	1914	97.87	697		ARO	546.
11	2095	92.45	687	5	8.1	544.
12	2518	98.10	640		ARO	546.
13	3397	92.	565	5	13.4	546.
14	3819	99.33	550		ARO	547.
15	3940	100.	510		ARO	547.
16	5000	100.	420		ARO	546.
17	6000	100.	330		ARO	546.
18	7000	100.	240		ARO	546.
19	8000	100.	150		ARO	546.
20	9000	100.	60		ARO	546.
21	9700	100.	1		ARO	546.
22	9700	100.	35		ARO	547.
23	9831	100.	35		ARO	547.

TABLE 4.7

ROCS MANEUVER STRUCTURE  
ST. LUCIE I CYCLE 1

Maneuver No.	Burnup (MWD/T)	Percent Power	PPM	Bank	Rod Position % In	Inlet Temp. °F
0	0	50	730		ARO	537
1	401	80	710		ARO	537
2	722	50	715		ARO	537
3	782	0	1020		ARO	532
4	817	30	730		ARO	535
5	1320	51	685		ARO	537
6	1320	81	635		ARO	540
7	1750	90	614		ARO	541
8	2190	100	590		ARO	542
9	3000	100	575		ARO	542
10	3440	95	570		ARO	542
11	4410	100	546		ARO	542
12	4900	100	533		ARO	542
13	5500	100	508		ARO	542
14	6000	100	488		ARO	542
15	6490	100	471		ARO	542
16	7000	100	453		ARO	542
17	7500	100	441		ARO	542
18	8000	100	424		ARO	542
19	8975	100	374		ARO	542
20	9500	100	348		ARO	542
21	9910	100	327	7		539
22	10305	100	314	7 <sup>+</sup>	3.	539
23	10590	100	295	7	17.	539
24	11360	100	249	7	5.	539
25	12376	100	188	7	5.	539

---

+ All other rods were at 3.4% insertion for the rest of the cycle.

TABLE 4.8

ROCS MANEUVER STRUCTURE  
ST. LUCIE I CYCLE 2

Maneuver No.	Burnup (MWD/T)	Percent Power	PPM	Rod Position Bank	% In	Inlet Temp. °F
0	0	50	850		ARO	542
1	0	30	850	7	5.	542
2	190	90	706	7	5.	542
3	308	98	697	7	7.	542
4	553	100	663	7	1.	542
5	553	100	661	7	9.	542
6	1050	100	619	7	9.	542
7	1359	100	597	7	1.	542
8	1726	100	584	7	3.	542
9	2238	100	550	7	1.	542
10	2361	85	531	7	3.	542
11	2731	100	496	7	1.	542
12	3142	100	476	7	3.	542
13	3662	100	434	7	1.	542
14	4093	100	403	7	1.	542
15	4216	0	1000	7	100.	542
16	4216	100	416	7	1.	542
17	4660	100	354	7	1.	542
18	4660	100	354	7	1.3	542
19	5095	100	308	7	1.3	542
20	5095	100	297	7	16.	542
21	5434	100	288	7	1.3	542
22	5959	100	245	7	1.3	542
23	6381	100	212	7	1.3	542
24	6472	0	700	7	100.	542
25	6472	100	186	7	1.3	542
26	7009	100	163	7	1.3	542
27	7363	100	139	7	1.3	542
28	7363	100	139	7	1.5	542
29	7860	100	102	7	1.5	542
30	8358	100	67	7	1.5	542

TABLE 4.9

ROCS MANEUVER STRUCTURE  
ST. LUCIE I CYCLE 3

Maneuver No.	Burnup (MWD/T)	Percent Power	PPM	Rod Position		Inlet Temp. °F
				Bank	% In	
0	0	76	800	ARO		538
1	484	100	764	ARO		541
2	1006	100	723	ARO		541
3	1430	100	690	ARO		541
4	1860	100	674	7	1.5	541
5	2379	100	632	7	2.2	541
6	2921	100	565	7	3.4	541
7	3393	100	536	7	3.4	541
8	3915	100	485	7	4.2	541
9	4519	100	440	7	4.2	541
10	5597	100	350	7	4.2	541
11	6674	100	260	7	4.2	541
12	7751	100	181	7	4.2	541

### Response to Question 13

In order to explain the interpolation scheme, replace the fourth sentence in the second paragraph on page 4.4 by the following:

"It is not feasible to perform an explicit reactivity calculation at each measured statepoint, but it is desirable to benefit from this large data base for the definition of a reactivity bias. An interpolation scheme was developed to use all the measured data to produce a large calculated reactivity data base. A measured (but not calculated) statepoint is characterized by an exposure lying between the exposures of two adjacent calculated statepoints. A linear interpolation is performed on all parameters of the calculated adjacent statepoints to produce an interpolated calculated statepoint at the exposure of the intermediate measured statepoint. The interpolated and measured statepoints may differ because of slightly different rod insertion, boron concentration, etc. A calculated reactivity correction is then applied to the interpolated statepoint to account for these differences, using calculated reactivity coefficients for the differential rod worth, boron worth, etc. A reactivity is thus calculated for the various measured critical statepoints during the cycle. The measured data and interpolation procedure with the calculated reactivity worths are only used for measured statepoints which lie between calculated statepoints at comparable power levels, rod insertions and moderator temperatures. Therefore, very nearly the same uncertainty is expected to apply to the calculated interpolated and basic calculated values. The uncertainty is evaluated for the aggregate of all points and therefore reflects any increase in uncertainty that might be due to the interpolation procedure."

Response to Question 14

In order to further discuss the reactivity behavior, replace the last sentence in the second paragraph on page 4.4 with the following:

"While there is a small downward trend with burnup in the low burnup ranges for first cycles, the reactivity level recovers in these cases to the average value by the end of cycle. The average bias for first cycles [ ] is only slightly lower than the average bias for all cycles [ ], and that for later cycles [ ]. The effect is sufficiently small that the cause has not been isolated."

Response to Question 15

Figures showing comparisons of measured and calculated radial and axial power distributions will be provided. To accomplish this, add the following after the last sentence in the last paragraph on page 4.7:

"Figures 4-2 through 4-9 show representative comparisons of the calculated and measured  $F_p$  values for each of the 8 reactor cycles near BOC. Figures 4-10 through 4-17 show the comparisons of the corresponding measured and calculated core average axial shapes for each of the cycles.

Figure 4-2  
COMPARISON OF MEASURED AND CALCULATED  
AXIALLY SUMMED RADIAL POWER DISTRIBUTION  
ANO-2 CYCLE 1 AT 2380 MWD/T

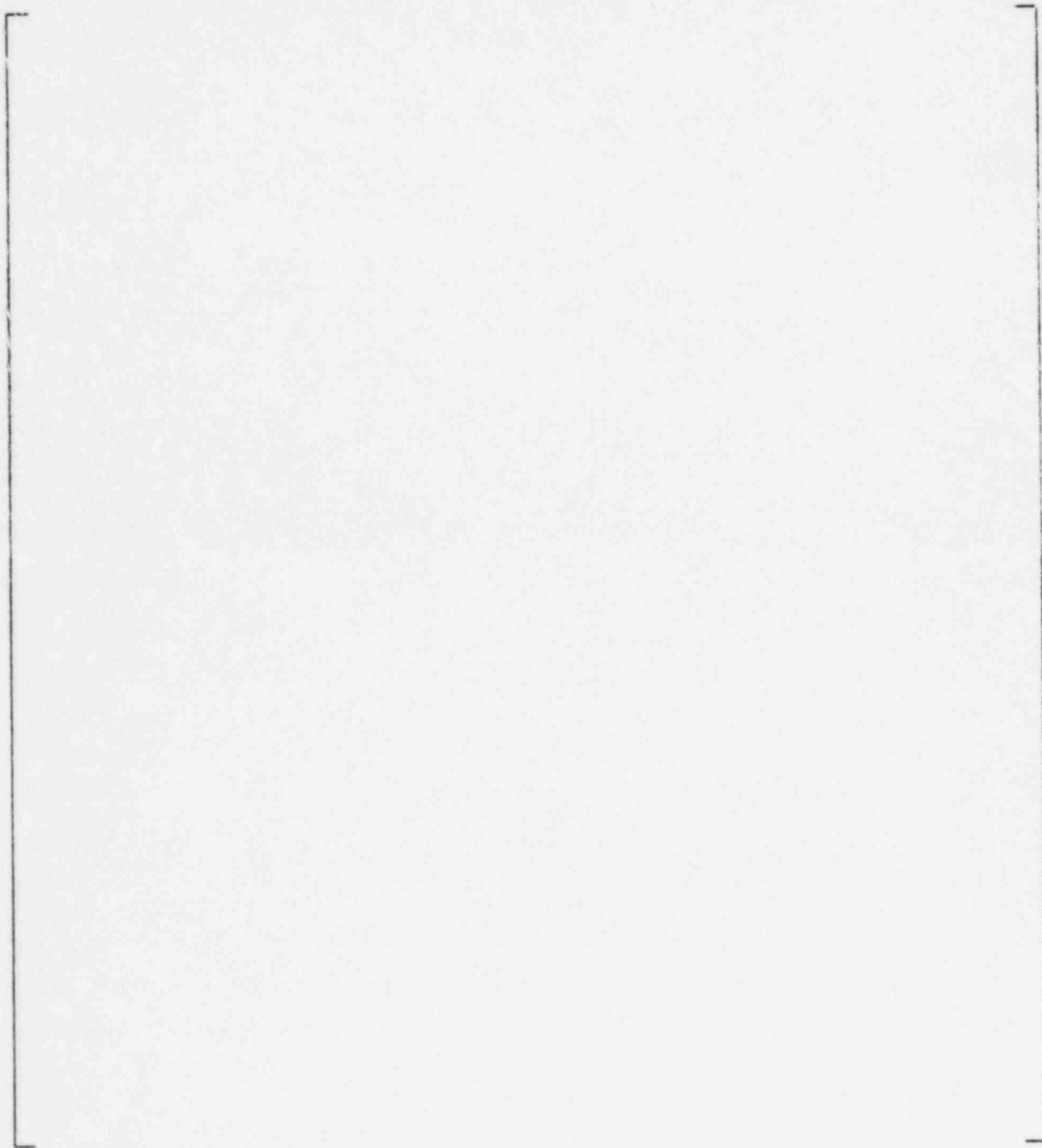


Figure 4-3  
COMPARISON OF MEASURED AND CALCULATED  
AXIALLY SUMMED RADIAL POWER DISTRIBUTION  
CALVERT CLIFFS 1 CYCLE 1 AT 850 MWD/T

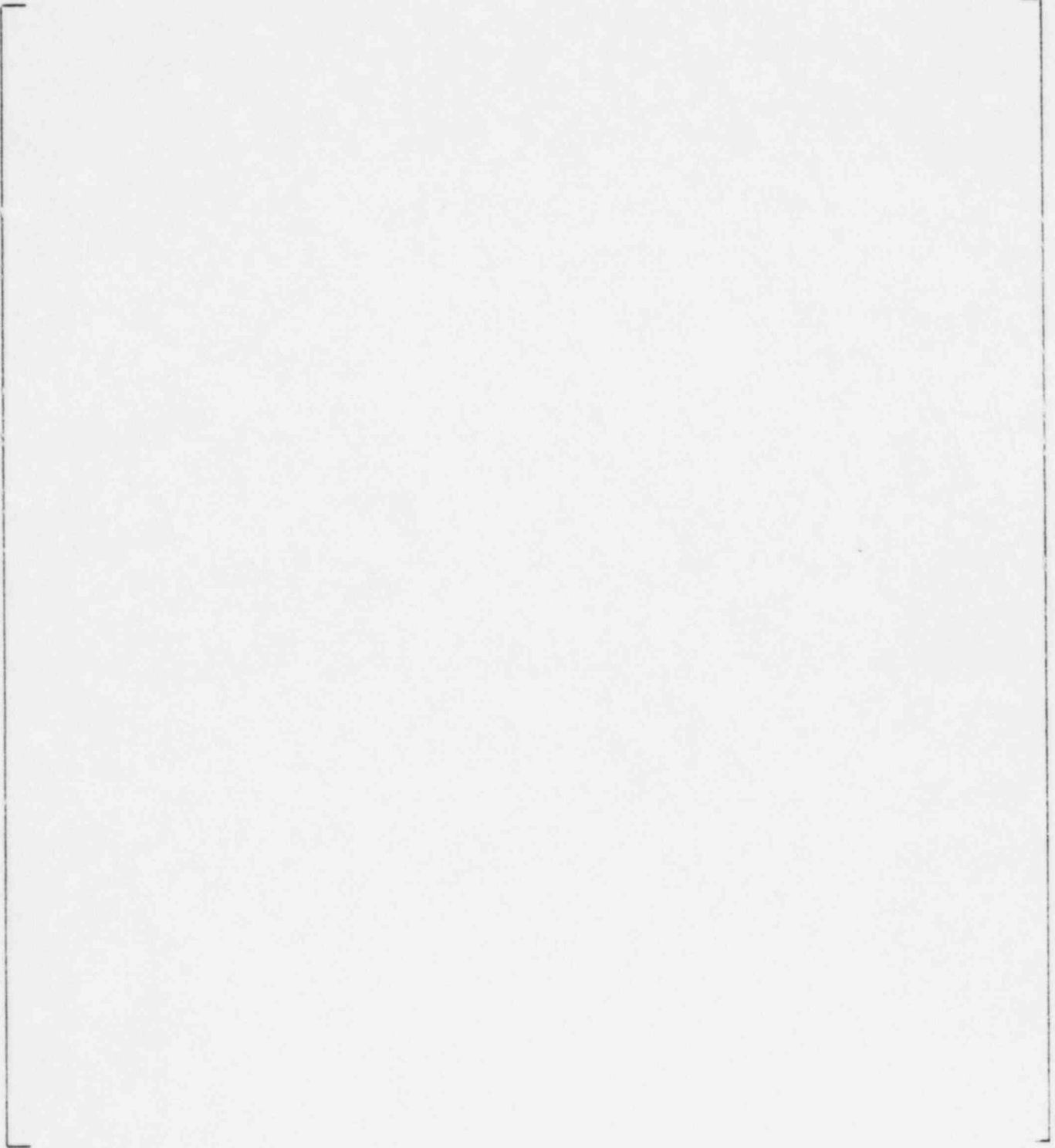


Figure 4-4  
COMPARISON OF MEASURED AND CALCULATED  
AXIALLY SUMMED RADIAL POWER DISTRIBUTION  
CALVERT CLIFFS 1 CYCLE 2 AT 332 MWD/T

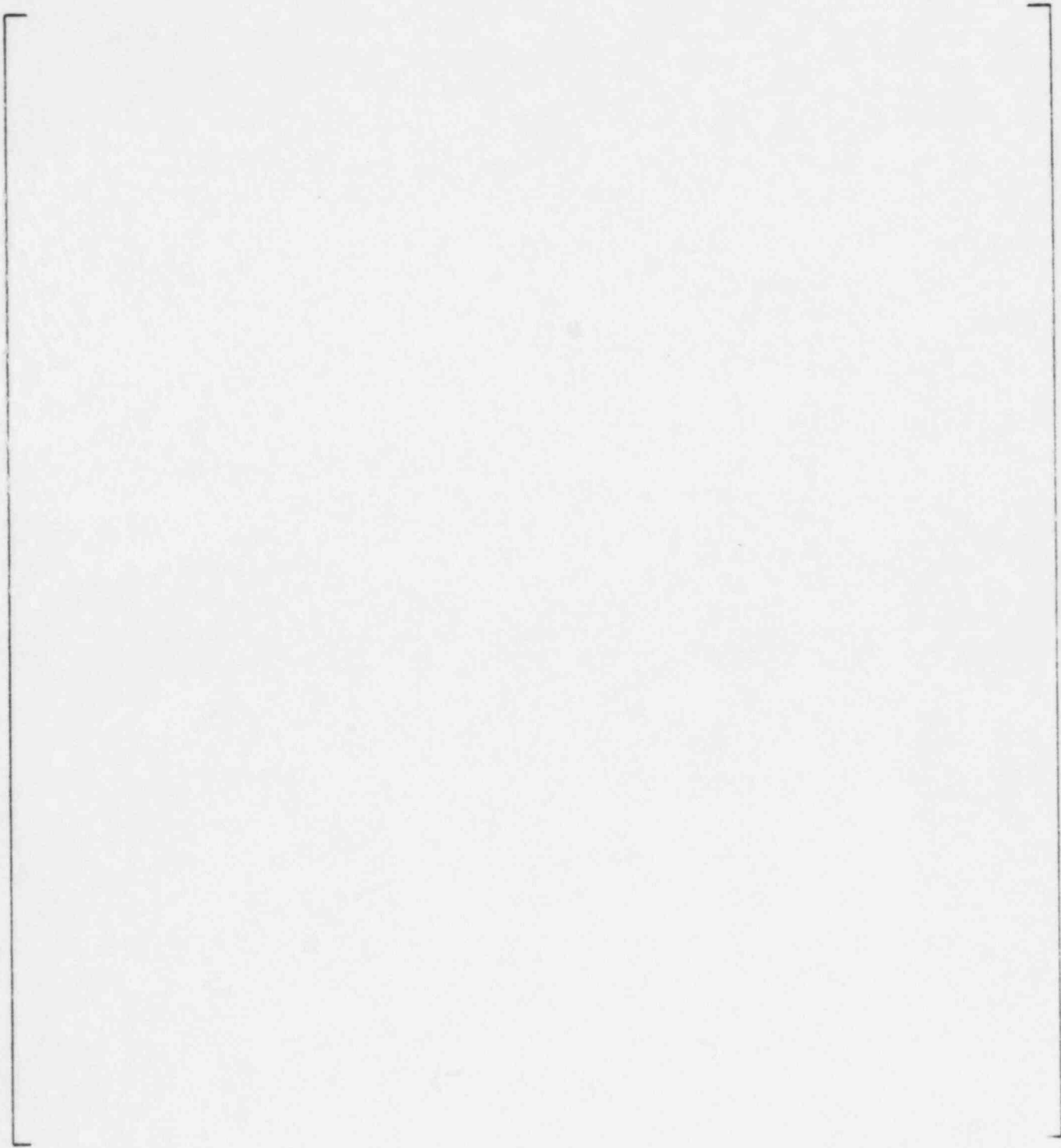


Figure 4-5  
COMPARISON OF MEASURED AND CALCULATED  
AXIALLY SUMMED RADIAL POWER DISTRIBUTION  
CALVERT CLIFFS II CYCLE 1 AT 1440 MWD/T

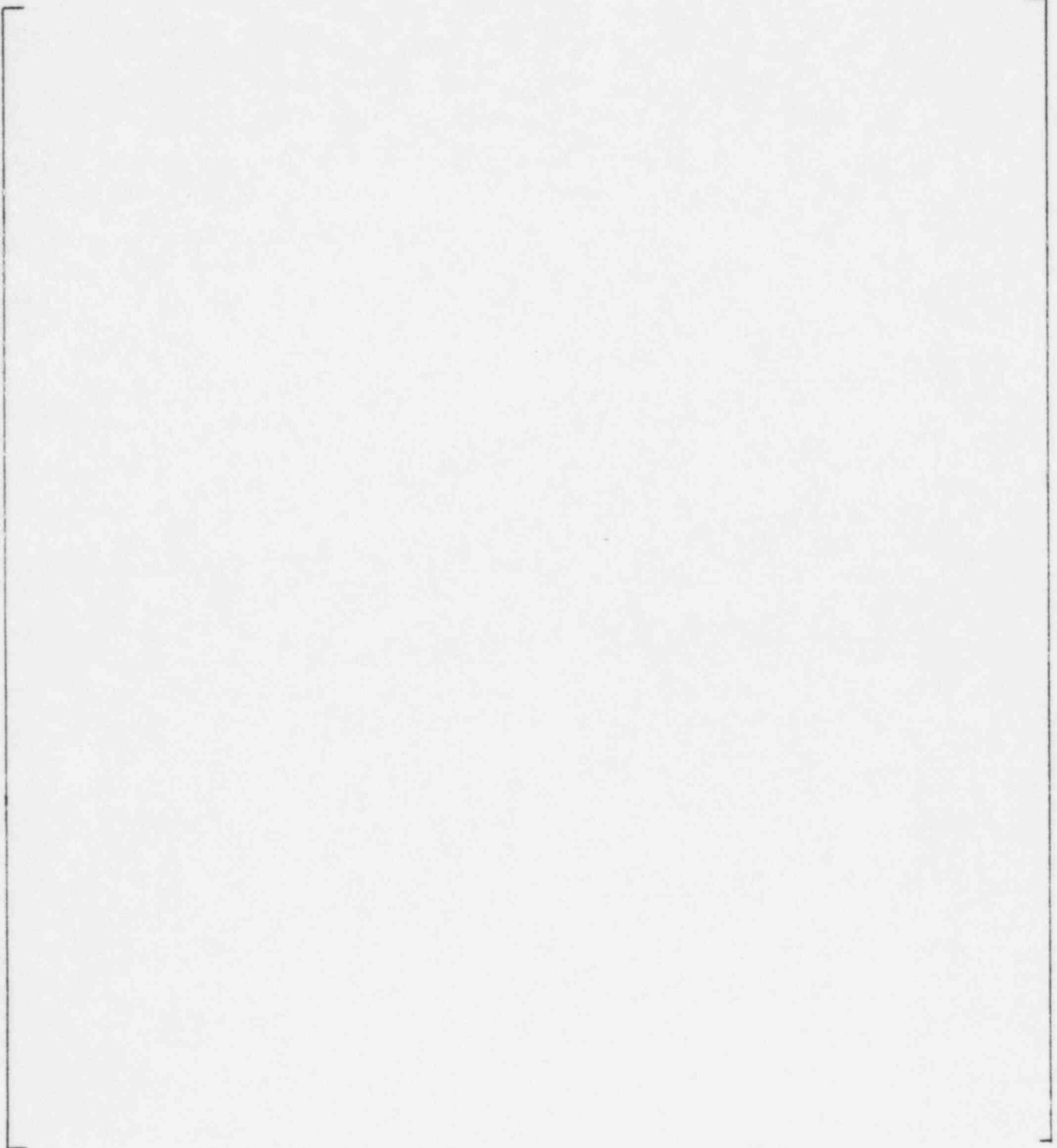


Figure 4-6  
COMPARISON OF MEASURED AND CALCULATED  
AXIALLY SUMMED RADIAL POWER DISTRIBUTION  
CALVERT CLIFFS II CYCLE 2 AT 1438 MWD/T

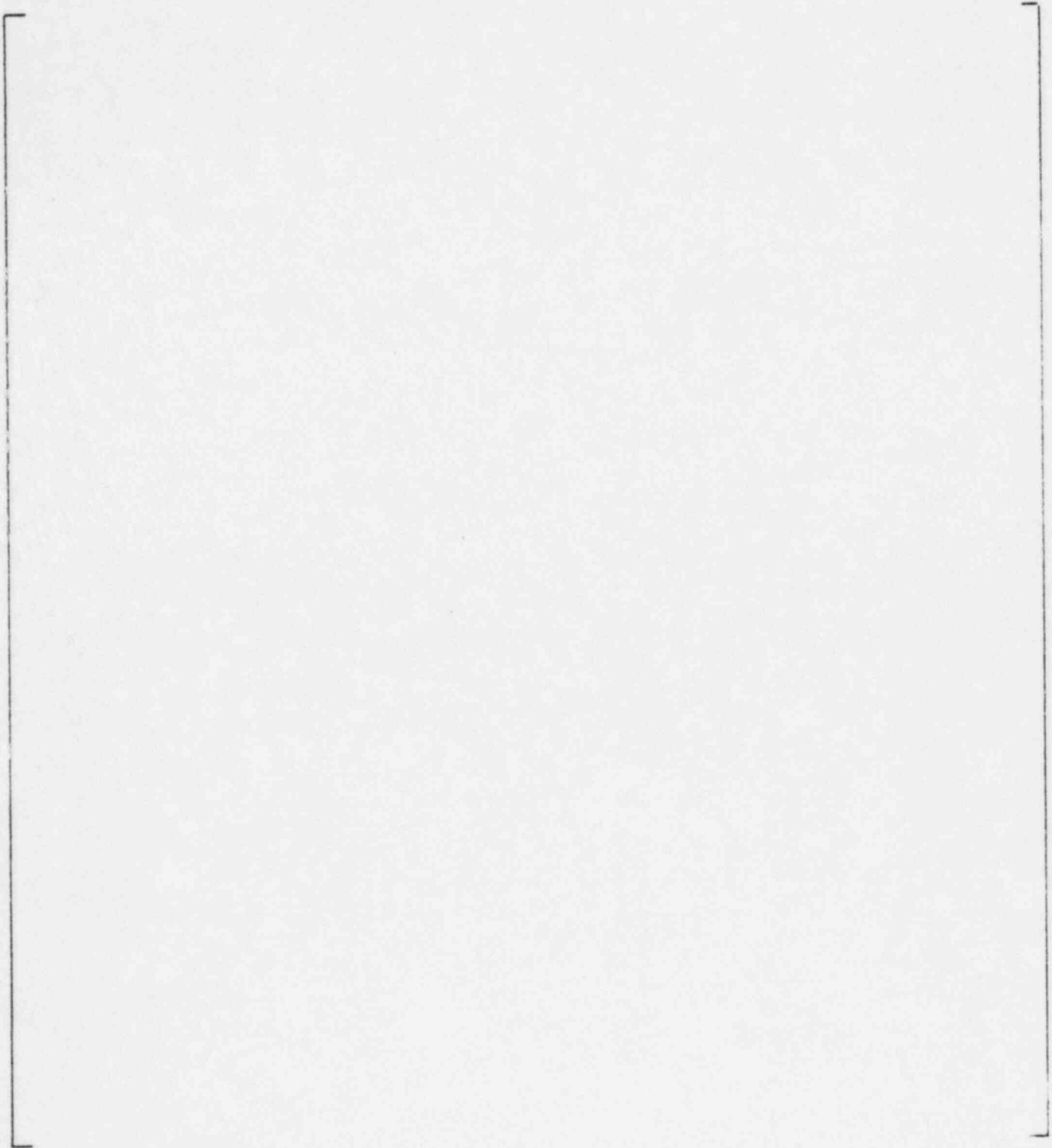


Figure 4-7  
COMPARISON OF MEASURED AND CALCULATED  
AXIALLY SUMMED RADIAL POWER DISTRIBUTION  
ST. LUCIE I CYCLE 1 AT 2139 MWD/T

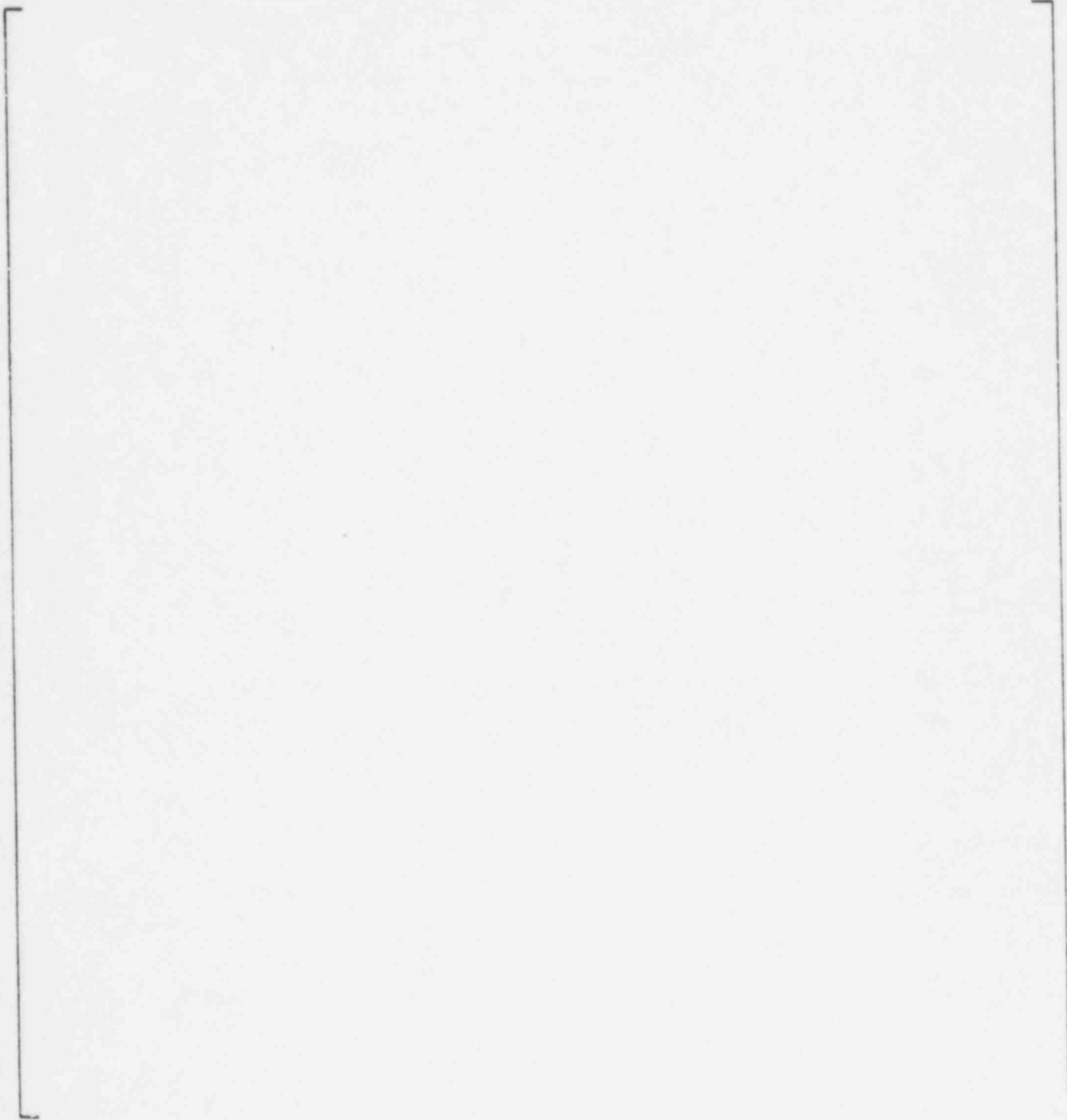


Figure 4-8  
COMPARISON OF MEASURED AND CALCULATED  
AXIALLY SUMMED RADIAL POWER DISTRIBUTION  
ST. LUCIE I CYCLE 2 AT 317 MWD/T

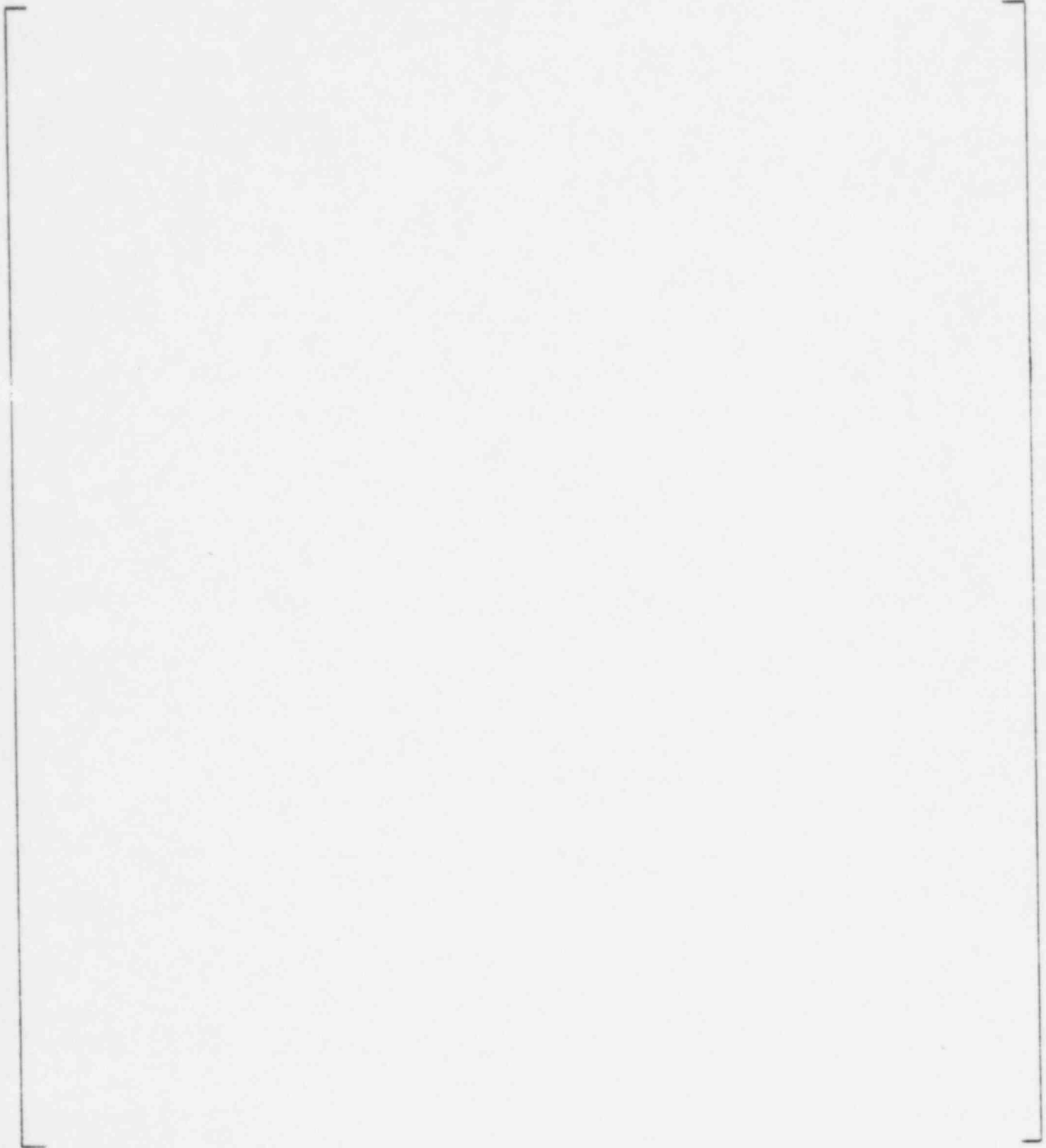


Figure 4-9  
COMPARISON OF MEASURED AND CALCULATED  
AXIALLY SUMMED RADIAL POWER DISTRIBUTION  
ST. LUCIE 1 CYCLE 3 AT 486 MWD/T

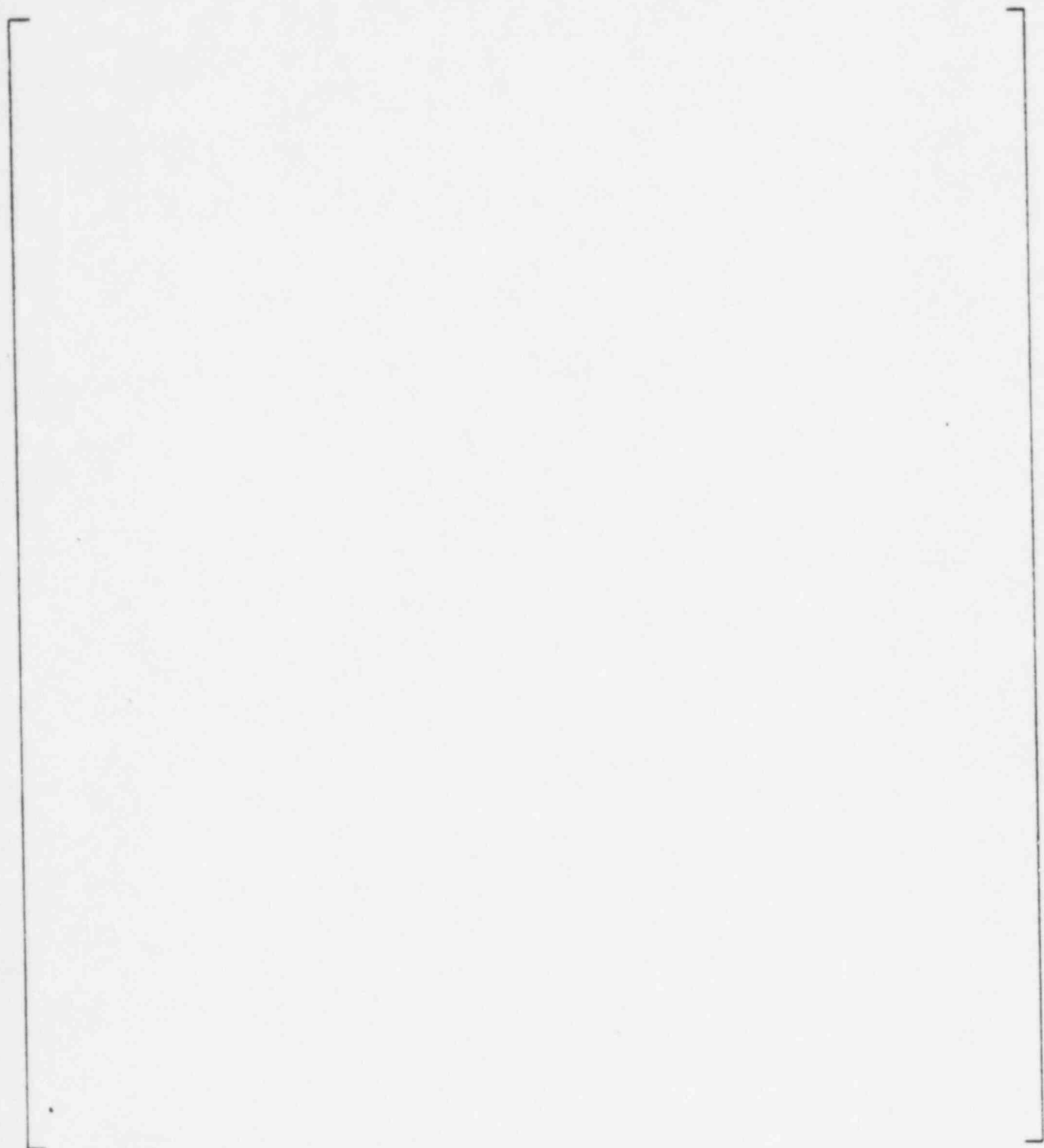


Figure 4-10  
ANO-2 CYCLE 1  
2380 MWD/T  
COMPARISON OF ROCS AND CECOR CORE AVERAGE AXIAL SHAPES



Figure 4-11  
CALVERT CLIFFS I CYCLE 1  
COMPARISON OF ROCS AND CECOR CORE AVERAGE AXIAL SHAPES  
880 MWD/T



Figure 4-12  
CALVERT CLIFFS 1 CYCLE 2  
COMPARISON OF ROCS AND CECOR CORE AVERAGE AXIAL SHAPES  
332 MWD/T



Figure 4-13  
CALVERT CLIFFS II CYCLE 1  
COMPARISON OF ROCS AND CECOR CORE AVERAGE AXIAL SHAPES  
1440 MWD/T



Figure 4-14  
CALVERT CLIFFS II CYCLE 2  
COMPARISON OF ROCS AND CECOR CORE AVERAGE AXIAL SHAPES  
1438 MWD/T



Figure 4-15  
ST. LUCIE I CYCLE 1  
COMPARISON OF ROCS AND CECOR CORE AVERAGE AXIAL SHAPES  
2139 MWD/T

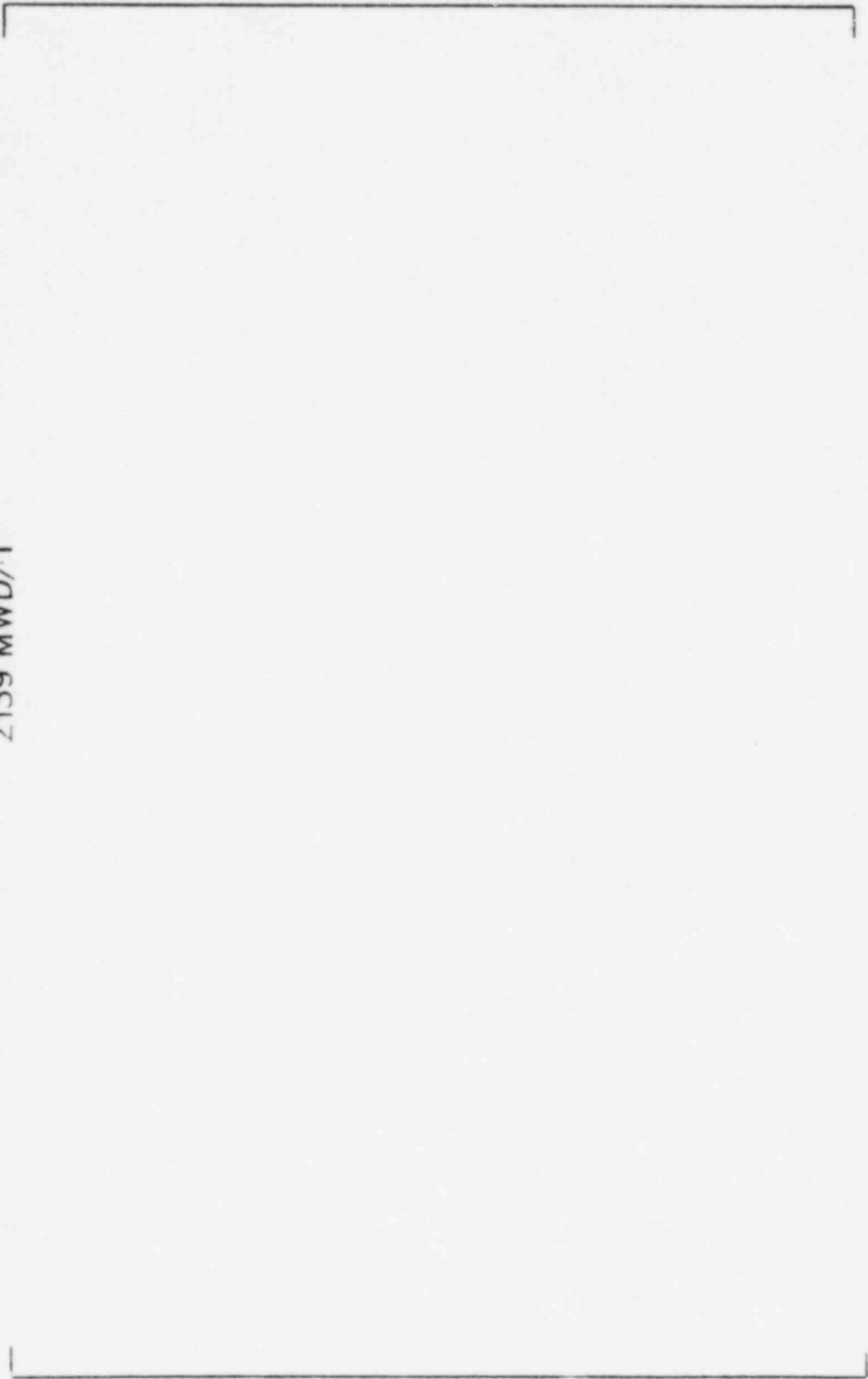
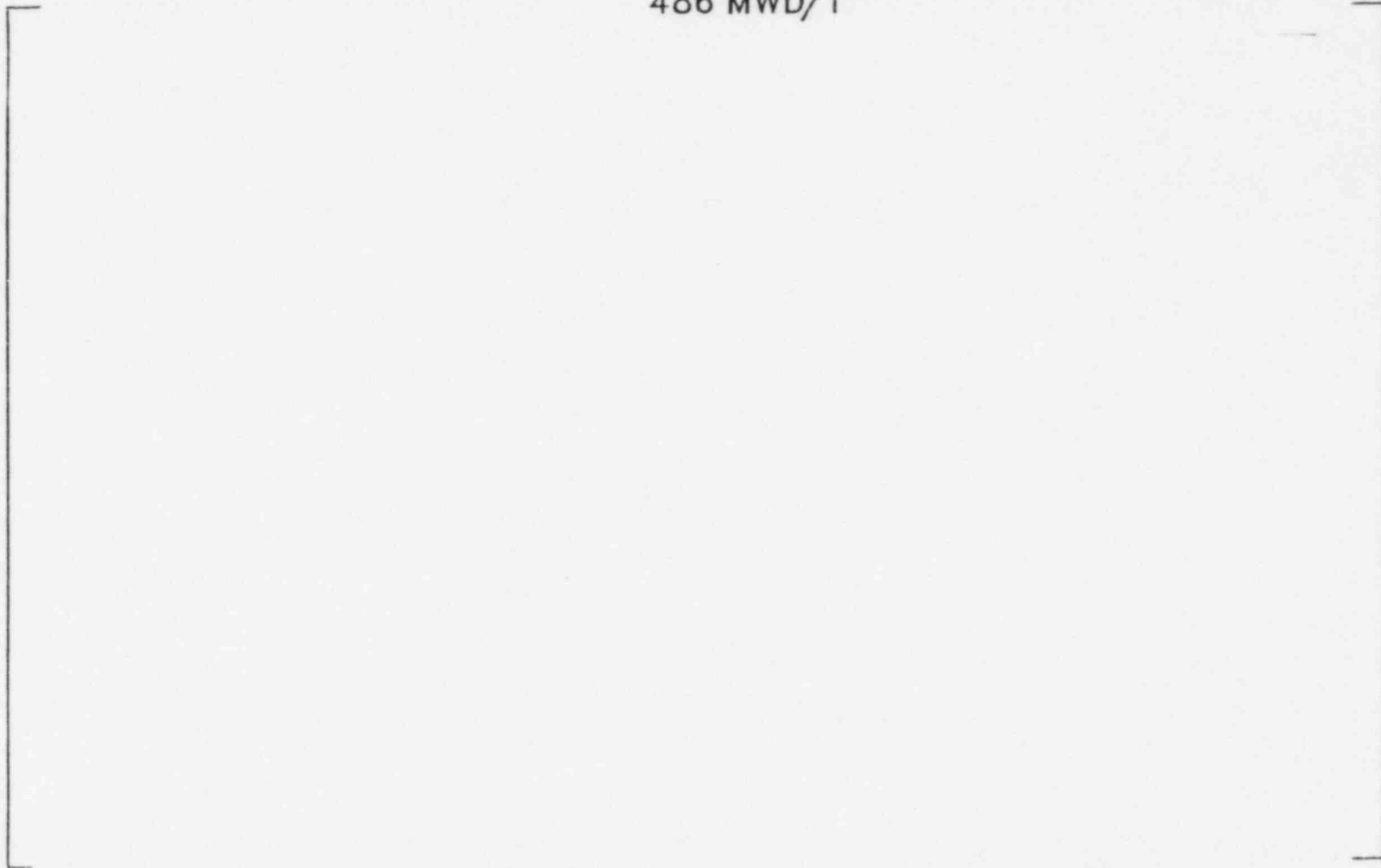


Figure 4-16  
ST. LUCIE I CYCLE 2  
COMPARISON OF ROCS AND CECOR CORE AVERAGE AXIAL SHAPES  
317 MWD/T



Figure 4-17  
ST. LUCIE I CYCLE 3  
COMPARISON OF ROCS AND CECOR CORE AVERAGE AXIAL SHAPES  
486 MWD/T





### Response to Question 17

The changes in macroscopic cross sections due to rods were obtained by taking the differences of assembly flux and volume weighted macroscopic cross sections for rodged and unrodged configurations from fine mesh PDQ calculations. The fine mesh rod cross sections were obtained with the CERES code which uses blackness theory and provides equivalent homogenized diffusion theory parameters for the CEAs in PDQ. An alternative procedure has been developed where the delta-macroscopic cross sections for ROCS are obtained directly from rodged and unrodged assembly calculations performed with the DIT code. This procedure is found to produce good results relative to measurements and relative to the PDQ/CERES calculative procedure, while requiring fewer job steps and facilitating the parameterization of rodged cross sections for ROCS. It is expected that the direct DIT procedure will be adopted in future licensing work. Section 4.1.5 will be revised to include the results from both methods. Since the bank worth agreement shows small differences between the two methods, the rod worths for upset conditions will not be recalculated, and the section will not be revised. The results for both methods are given below in the revised tables.

In order to clarify the procedure currently used and to describe the new method replace the second paragraph of Section 4.1.5 on page 4.14 with the following.

"Homogenized cross sections used in the rod worth calculations were obtained [

In addition, insert the following references on page 4.25 and renumber the rest.

- "4.2 Stuart, G. W. and Woodruff, R. W., "Method of Successive Generations," Nucl. Sci. and Eng., 3, p 339 (1958).
- 4.3 Kear, G. N. and Ruderman, M. J., "An Analysis of Methods in Control Rod Theory and Comparison with Experiment," GEAP-3937 (May 1962).
- 4.4 Wachpress, E. L., "Thin Regions in Diffusion Theory Calculations," Nucl. Sci. and Eng., 3, p 186 (1958).
- 4.5 Henry, A. F., "A Theoretical Method for Determining the Worth of Control Rods," WAPD-218 (August 1959)."

Calculations have been made comparing the results with the PDQ/CERES and direct DIT methods. The revised Tables 4.19 and 4.22 with the results of both methods are given below. Sections 4.1.5 and 6.0 will be revised accordingly. Both procedures have been used for design and operation now being licensed, while the transition to the new method is under way.

TABLE 4.19

ROD BANK WORTH SUMMARY FOR ROCS/DIT  
MEANS & STANDARD DEVIATIONS

<u>Sample Description</u>	$\bar{x}$	$S_D$	$S_M$	$S_C$
Units of % of Bank Worth				
PDQ/CERES METHOD:				
First Cycles	[			]
Reload Cycles	[		-	]
DIRECT DIT METHOD:				
First Cycles	[			]
Reload Cycles	[			]

TABLE 4.22

BEST ESTIMATED ROD WORTH BIASES AND UNCERTAINTIES FOR ROCS/DIT

Units of % of Bank Worth

	<u>Bias Observed</u>	<u>Uncertainties</u> *	
Individual Banks	X	kS <sub>D</sub>	kS <sub>C</sub>
PDQ/CERES METHOD			
First Cycles	[		]
Reload Cycles	[		]
DIRECT DIT METHOD			
First Cycles	[		]
Reload Cycles	[		]

---

\* 95/95 Probability/confidence level

Response to Question 18

The individual measured and calculated values, as well as the differences, will be provided for both methods. To accomplish this, replace the present Table 4.18 with Tables 4.18A and 4.18B.

TABLE 4.18 A.1  
 COMPARISON OF CONTROL ROD BANK WORTHS  
 CALCULATED (C) 3D ROCS (DIT) vs MEASURED (M)  
 PDD/CERES METHOD  
 $\% \Delta \rho$

PLANT/CYCLE	ANO 2	C.C.I	C.C.II	St.L.I
SEQUENTIAL ROD BANK	CY 1	CY 1	CY 1	CY 1
FIRST CYCLES	C M	C M	C M	C M
LATER CYCLES	C C.I CY 2	C.C.II CY 2	St.L.I CY 2	C.C.I CY 3
	C M	C M	C M	C M
				C.C.I CY 4
				St.L.I CY 3
				C M
				C M
				C M
				C M







Response to Question 19 and 20

Both questions deal with the calculation of reactivity worths for upset conditions and can be answered together. The choice of 2D or 3D models used in the dropped and ejected rod power distribution analysis is given in the third paragraph of section 4.2.2, page 4.22. To further explain the calculations, make the following changes:

Replace the last sentence in the last paragraph in Section 4.2 page 4-18 with the following:

"All calculations were performed in a full core geometry. Calculations in which control rod banks were either fully inserted or withdrawn, and in which no part-length rods were used, were performed in two dimensions. Calculations requiring the insertion of part length rods, or the ejection of a rod from a partially inserted bank, were run in three dimensions."

Add the following at the end of 1st paragraph on Section 4.2.1 on page 4-19:

"All the data analyzed were obtained during the start-up test programs of first cycles. Zero power data was strictly at beginning of cycle, whereas at power data were obtained during the power ascension phase, in a slightly depleted core. The critical statepoints prevailing during the measurements were reproduced in the calculational model."

Replace the second sentence of the first paragraph in the Dropped Rod Worths section on Page 4.19 by

"Two dimensional ROCS/DIT calculations were used for all cases except for the part length rod drop cases of ANO-2, which were calculated in three-dimensions. With the exception of the Calvert-Cliffs and Millstone II cases which were at 50% power, all dropped rod cases were at beginning of cycle, zero power."

Delete the second and third sentences of the first paragraph in the Ejected Rod Worths Section on pages 4.19 and 4.20, and replace by:

"Three dimensional full core calculations were used to analyze all measurements for both the reactivity worth and power distribution determination. The Calvert Cliffs data was taken at 20% power and one St. Lucie case was taken at 50% power. All other ejected rod cases were at zero power. All were at BOC."

Add the following second paragraph to the Net Rod Worth Section on page 4.20:

"The measured net rod worth is obtained as the sum of all regulating bank worths and of the first shutdown bank described in Section 4.1.5, to which the dropped worth of the last bank minus the stuck rod is added. The calculated worth is obtained similarly by combining the worth of each bank. All net worth cases were obtained at beginning of first cycles at zero power."

## Response to Question 21

Dropped, pseudo-ejected and net (N-1) CEA worth measurements are not performed for reload cores. It is generally assumed that the meeting of acceptance criteria in first cycle tests provides sufficient verification of calculational models. The conclusions in Section 4.2.1 rests in part, upon the consistency between upset rod configuration results and normal symmetric CEA bank insertions. That is, since there is no observed deterioration in the ROCS/DIT CEA worths for asymmetric (as opposed to symmetric) configurations in first cores, the quality of results for asymmetric configurations in reload cores would also be consistent with with the appropriate results of Section 4.1.5.

An expanded version of the original text is attached, and should replace page 4.21:

"The dropped, ejected and net rod worth comparisons all showed similar good results which are consistent with the previous analysis of control rod bank worths. This is demonstrated in Table 4.27 where the means and standard deviations for the upset rod configurations are compared with reactivity results for normal sequential insertions of control rod banks from Section 4.1.5. The normal rod bank reactivity results are taken from the first cycle only calculations seen in Table 4.18 because all upset rod calculations here were for first cycles. The mean and standard deviation for the normal sequential insertions are shown both in terms of relative differences (taken directly from Table 4.18) and the corresponding absolute reactivity differences. The rod drop and rod ejection results are shown in Table 4.27 in absolute units because relative units can be misleading when comparing small reactivity worths. The net (N-1) rod worth mean difference and standard deviation are show in Table 4.27 in relative terms. This mixed approach is consistent with the selection of acceptance criteria for C-E start-up measurements of control rod worths.

"Dropped, ejected and net rod worth measurements are only performed for first cycles. The meeting of the acceptance criteria during first cycle startup tests provides sufficient verification of calculational models. Table 4.27 shows that the results obtained here for upset conditions compare in first cycles favorably with the calculations for normal control rod operation in first cycles. The mean differences are similar, showing basically a small underprediction of the measured rod worths. The standard deviations for the upset rod configurations are either less than or equal to the parallel symmetric rod bank results. That is, there is no observed deterioration in the ROCS/DIT rod worths for asymmetric rod configurations. Since the asymmetric results here are consistent with the normal sequential rod insertion results for first cycles, it is reasonable to expect that the quality of results for asymmetric calculations in reload cores would also be consistent with the appropriate results of Section 4.1.5. Thus the maximum control rod worth calculational uncertainty value of [ ] taken from Table 4.22 of Section 4.1.5 would be a conservative choice to envelope upset rod configuration calculations regardless of cycle. The appropriate cycle dependent biases from Table 4.22 will be used for first and later cycles, respectively, or the more conservative value for a particular application may be used."

Response to Question 22

The prompt thermal hydraulic feedbacks that were used for the analyses of Section 4.2.2. were fuel temperature (Doppler) and moderator density feedbacks. To further explain this replace the next to last sentence in third paragraph of Section 4.2.2 on page 4.22 with the following:

"All ROCS calculations simulated [

]"

Response to Question 23

As a conservative measure, the worst case cycle/reactor data from Tables 4.11 through 4.13, summarized in Table 4.14, were used for the ROCS/DIT box power calculative uncertainty. To further clarify the statements on pp 4.10, 5.1, 5.2 add the following after the first sentence in Section 5.2 on page 5.7.

"The box values are from Table 4.14 in Section 4.1.2 and represent the worst values for all reactors and cycles. Similarly, the pin/box values were calculated in Section 5.1 using the least favorable, BOC, rodged MC case from Table 2.2 in Section 2.5.4.

Ts5006  
WBT/lf